SoftCOM '18
tutorials

Structuring Electromagnetic Problems – A Clear Path in the Design of Electromagnetic Structures

by

Zvonimir Šipuš

University of Zagreb, Croatia

September 13 - 15, 2018.

Structuring Electromagnetic Problems

A Clear Path in the Design of Electromagnetic Structures

Zvonimir Šipuš
University of Zagreb

Per-Simon Kildal (1951-2016)

Outline

- Motivation
- Canonical surfaces, EBG surfaces, soft and hard surfaces
- Applications
- Modelling of EM surfaces
- G1DMULT and G2DMULT algorithms
- Story about cloaking

Motivation

- Natural way of designing devices:

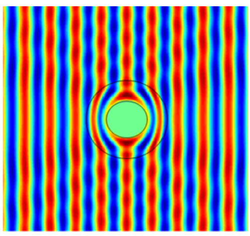

Concept development

↓

Device development

↓

Practical realization

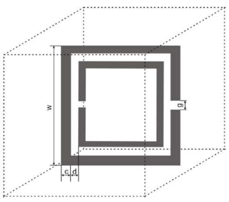

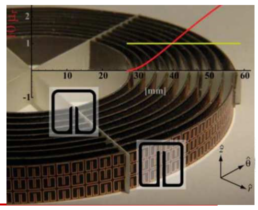

Canonical surfaces

Canonical Surface		E-field Polarization	
		VER or TM	HOR or TE
PEC		GO	STOP
PMC		STOP	GO
PEC/PMC Strip grid	SOFT	STOP	STOP
	HARD	GO	GO
PMC-type EBG	grazing	STOP	STOP
	close to normal	PMC	

2005: IEEE Transactions Special Issue with Table
for comparing surfaces with respect to surface waves.

Explanations of Abbreviations

- GO surfaces: Enhances propagation of waves along surface
- STOP surface: Stops propagation of waves along surface
- PEC = Perfect Electric Conductor
- PMC = Perfect Magnetic Conductor
- AMC = Artificial Magnetic Conductor
- PBG = Photonic Bandgap Material
- EBG = Electromagnetic Bandgap Material
- EMXtals = Electromagnetic Crystals

Canonical surfaces

Two fundamental questions:

- Can we make a low-profile antennas?

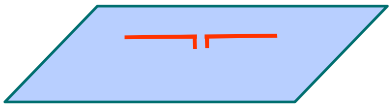

- Can the EM wave propagate along the surface?

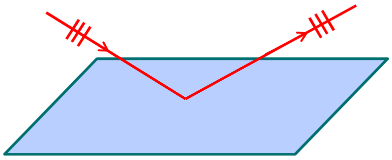

PEC: Wave propagation along surface

VER propagation GOes with

$$\partial E_{VER} / \partial n = 0$$

at surface.

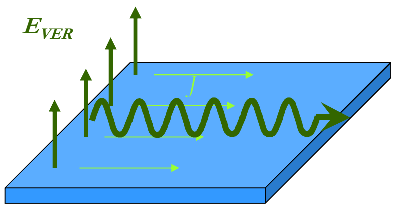

HOR polarization STOPs with

$$E_{HOR} = 0$$

at surface

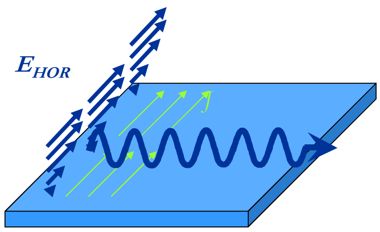

Picture: P.-S. Kildal

The PEC canonical surface (Perfect Electric Conductor)

- Commonly used in almost all microwave and antenna analysis of metal conductors
- Characteristics:
  - "Short circuits" electric current sources
  - VER polarization **GO**es along PEC (longitudinal electric currents make waves go)
  - HOR polarization **STOP**s along PEC (transverse electric currents stop waves)

The PMC canonical surface (Perfect Magnetic Conductor)

- Commonly used in theoretical works
- Commonly used as symmetry plane in some codes
- Characteristics:
  - Allows electric current sources at surface
  - HOR polarization **GO**es along PMC (longitudinal magnetic currents make waves go)
  - VER polarization **STOP**s along PMC (transverse magnetic currents stop waves)

The EM concept of soft and hard surfaces dates back to 1988 (Kildal) renewed interest in 1999 (Sievenpiper)

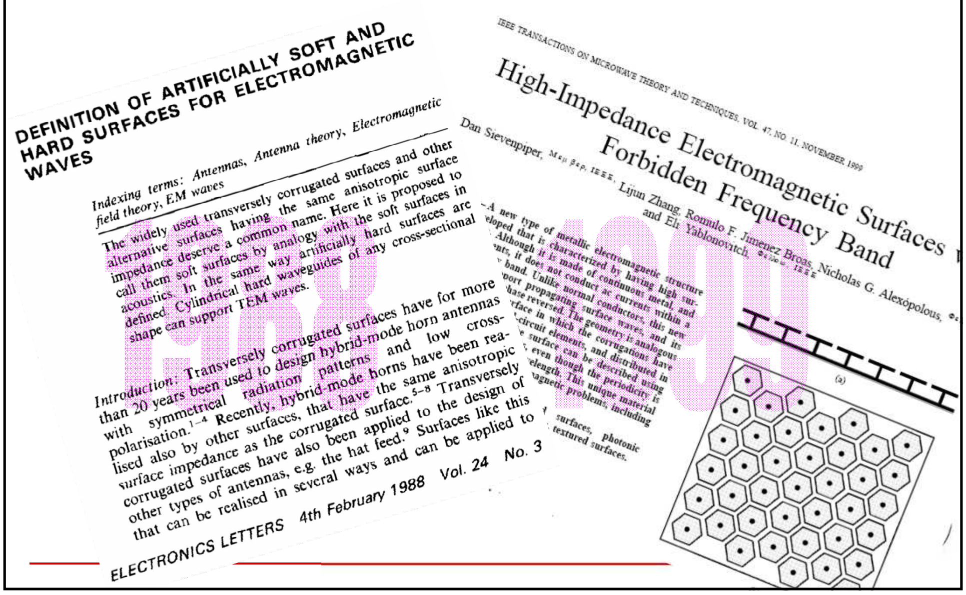

Canonical surfaces

- Soft and hard surfaces originate from acoustics and diffraction theory
- *p* is acoustic pressure

Surface	Boundary condition	Wave propagating at surface
Soft	$p = 0$	No
Hard	$\frac{\partial p}{\partial n} = 0$	Yes

Artificially soft and hard surfaces in electromagnetics

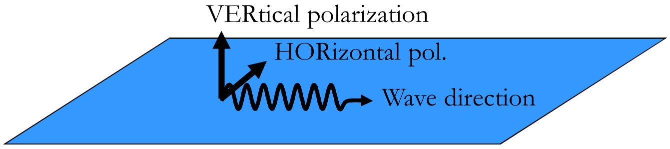

Type of surface	Boundary condition	Wave propagation at surface
Smooth conductor	$E_{HOR} = 0$ $\partial E_{VER} / \partial n = 0$	**STOP for HOR pol.** **GO for VER pol.**
Soft surface	$E_{HOR} = 0$ $E_{VER} = 0$	**STOP for HOR pol.** **STOP for VER pol.**
Hard surface	$\partial E_{HOR} / \partial n = 0$ $\partial E_{VER} / \partial n = 0$	**GO for HOR pol.** **GO for VER pol.**

Concept of soft and hard surfaces

- Soft surface: $E_n = 0,\ E_t = 0$
- Hard surface: $\partial E_n / \partial n \approx 0,\ \ \partial E_t / \partial n \approx 0$

In principal:

- A soft surface is a surface along which the power density of a propagating wave is zero.
  (**STOP** surface for both polarizations)
- A hard surface is a surface along which the power density of a propagating wave has a maximum.
  (**GO** surface for both polarizations)

Canonical surface: PEC/PMC strip grid

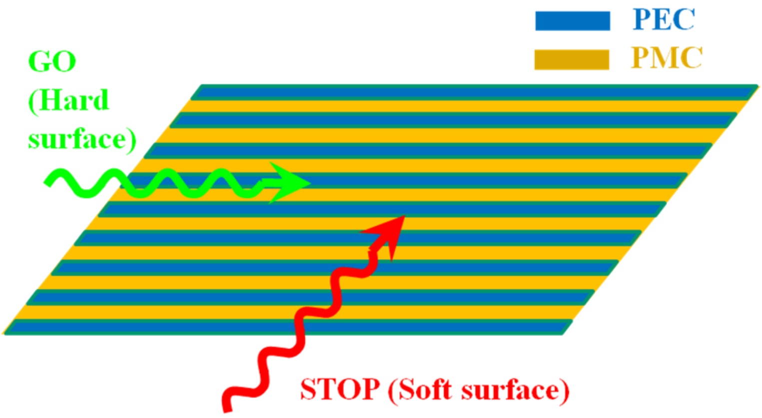

PEC/PMC strip surface

- Ideal soft surface = **STOP** surface
  - Current fences **stop** waves
- Ideal hard surface = **GO** surface
  - Current lanes let waves **GO**

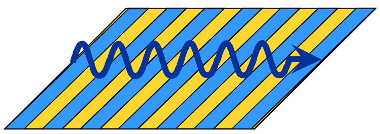

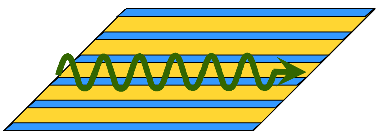

$$strip\ period \rightarrow 0$$

Picture: P.-S. Kildal

Realization of soft and hard surfaces with corrugations

Soft STOP surface

Hard GO surface

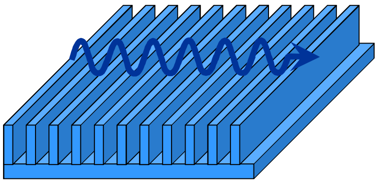

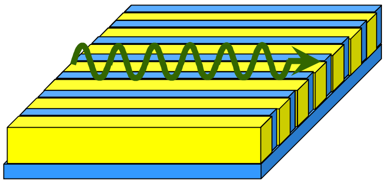

Transverse air-filled corrugations

Longitudinal dielectric-filled corrugations

Picture: P.-S. Kildal

Alternative realization: strip-loaded grounded substrate

Soft STOP surface

Hard GO surface

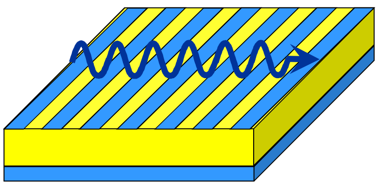

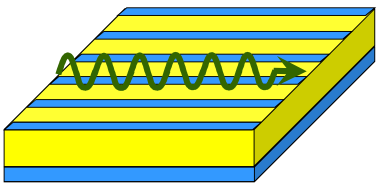

Picture: P.-S. Kildal

Soft surface: Principle of operation for transverse corrugations (current fences)

E_{VER} sees AMC (transformation from short-circuit to open-circuit in grooves)

$$E_{VER} = 0$$
$$J_{long} = 0$$

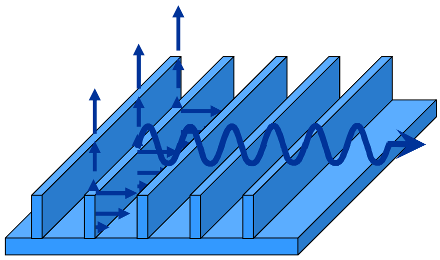

E_{HOR} sees PEC. No penetration into grooves.

$$E_{HOR} = 0$$
$$J_{transv} = undesturbed$$

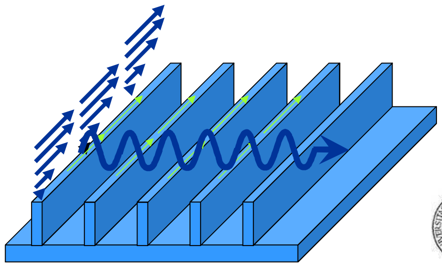

Picture: P.-S. Kildal

Soft surface: Bandwidth is limited by surface waves

Ideally large 2:1 bandwidth

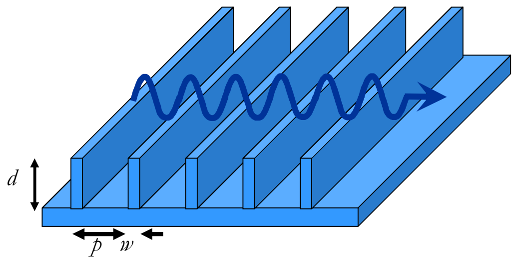

$$p < \lambda/2, \quad p/w < 2$$
$$\lambda_c = \text{wavelength in corrugations}$$
$$d < \lambda_c/4 \quad : \text{ surface waves}$$
$$\lambda_c/4 < d < \lambda_c/2 \quad : \text{ no surface waves, i.e. STOP band}$$
$$d = \lambda_c/4 \quad : \text{ best frequency}$$
$$d > \lambda_c/2 \quad : \text{ surface waves}$$

Picture: P.-S. Kildal

Soft surfaces

- Different forms of corrugations

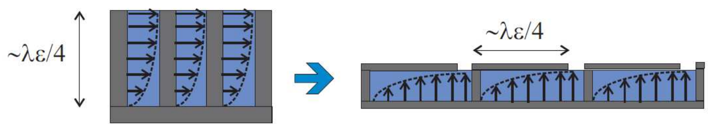

- Strip-loaded corrugations

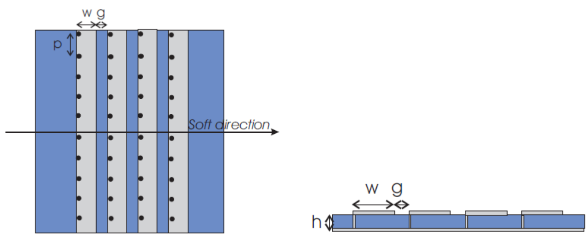

Picture: Eva Rajo-Iglesias

Comparison with respect to propagation of waves along the surface (surface waves)

Canonical Surface		E-field Polarization	
		VER or TM	HOR or TE
PEC		GO	STOP
PMC		STOP	GO
PEC/PMC Strip grid	SOFT	STOP	STOP
	HARD	GO	GO
PMC-type EBG	grazing	STOP	STOP
	close to normal	PMC	

EBG (Electromagnetic bandgap) surface

Sievenpiper 1999:
Mushroom surface

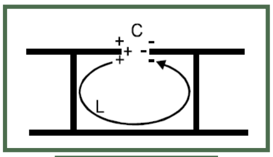

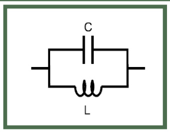

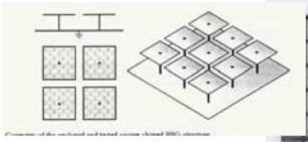

High impedance surface
=
Artificial Magnetic
Conductor (AMC)

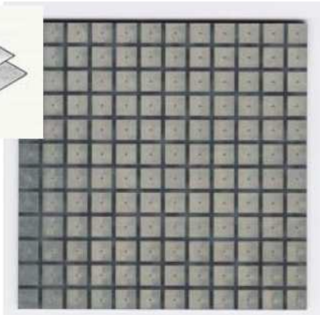

Very easy to model as a LC resonator. ➔ Increasing L or C the operation frequency will decrease

EBG surface

- Dispersion diagram:

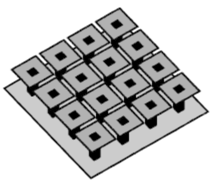

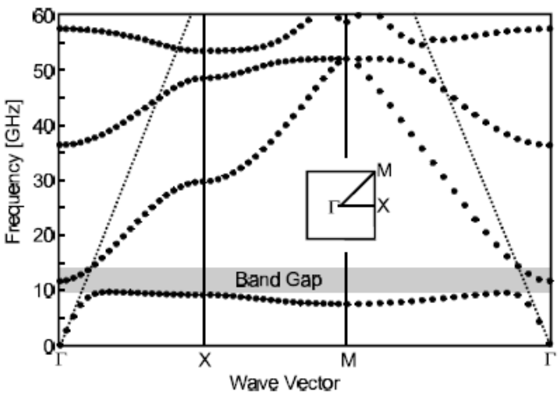

Figure 6.1.2 Surface wave band structure for a two-layer, high-impedance surface

Picture: Dan Sievenpiper

EBG surface

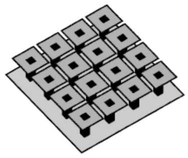

- Surface wave measurements:

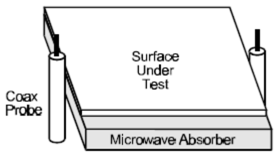

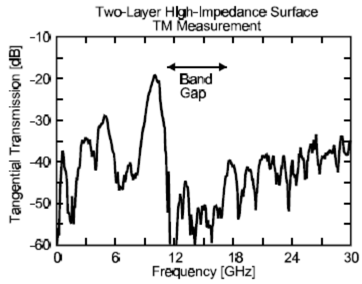

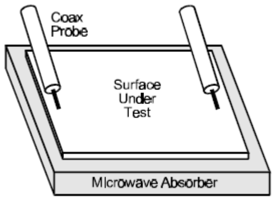

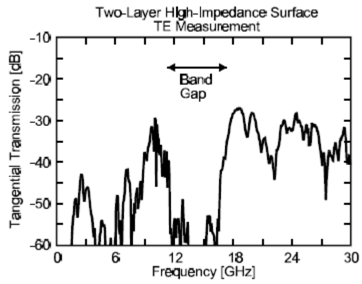

Picture: Dan Sievenpiper

EBG surface - About compactness

[Iluz et al.
IEEE TAP, 2004]

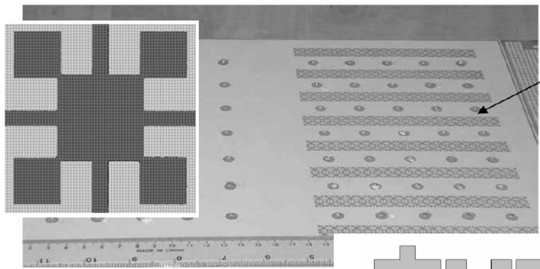

[Yang et al.
IEEE MTT, 2005]

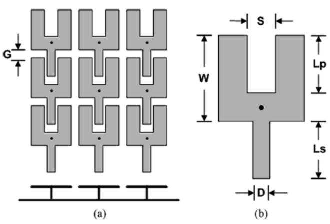

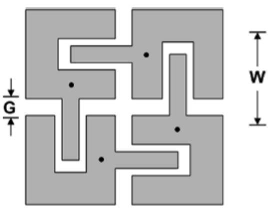

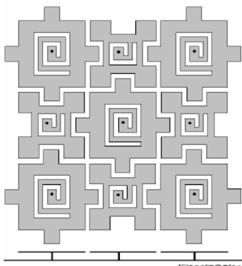

Canonical surfaces

Canonical Surface		E-field Polarization	
		VER or TM	HOR or TE
PEC		GO	STOP
PMC		STOP	GO
PEC/PMC Strip grid	SOFT	STOP	STOP
	HARD	GO	GO
PMC-type EBG	grazing	STOP	STOP
	close to normal	PMC	

Characterization of EBG surfaces

- The EBG surface we can characterize in different ways:
  - By dispersion diagram
  - By reflection coefficient of the incoming plane wave
  - By mutual coupling level between two antennas located above the EBG surface
  - By radiation pattern of an antenna located above the EBG surface
  - By input impedance of an antenna located above the EBG surface
- NOTE: different characterizations will determine different frequency bandwidths of interest.

Dimensions of mushroom structure and corrugated surface

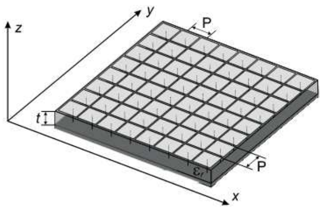

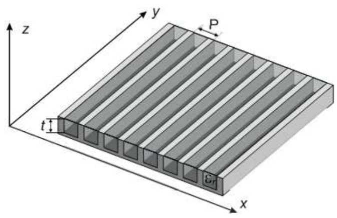

Mushroom structure:
- patches: 2.25x2.25 mm^2
- diameter of vias: 0.36 mm
- lattice constant: 2.4 mm
- dielectric: ε_r = 2.2,
  h = 1.6 mm

Corrugated surface:
- width/period = 0.9
- dielectric: ε_r = 2.2,
  h = 4.6 mm

Dispersion diagram of mushroom surface

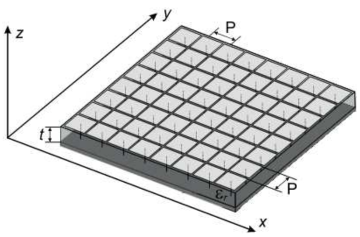

Mushroom structure:
- patches: 2.25x2.25 mm^2
- diameter of vias: 0.36 mm
- lattice constant: 2.4 mm
- dielectric: ε_r = 2.2,
  h = 1.6 mm

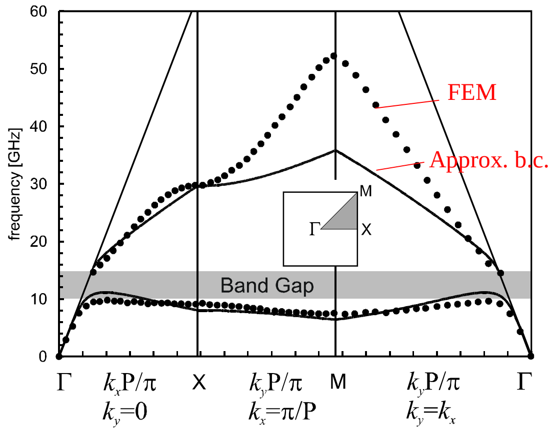

FEM Results by D. Sievenpiper, IEEE MTT 1999.

Comparison of mushroom surface and corrugated surface (STOP direction)

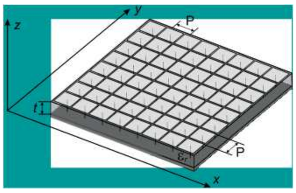

Stop band: 11.14 – 15.17 GHz

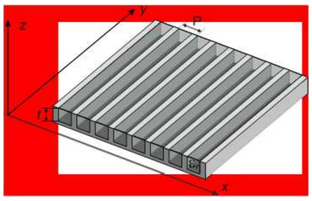

Stop band: 11.0 – 22.0 GHz

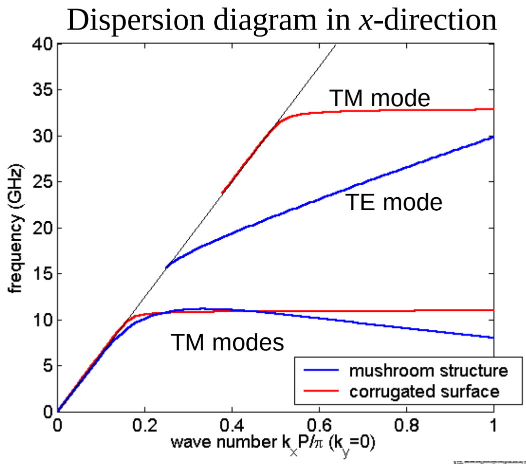

Horizontal dipole – mutual coupling

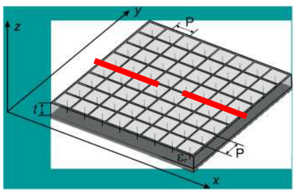

Dipoles:

- length: 10 mm
- height: 0.5 mm
- separation: 50 mm

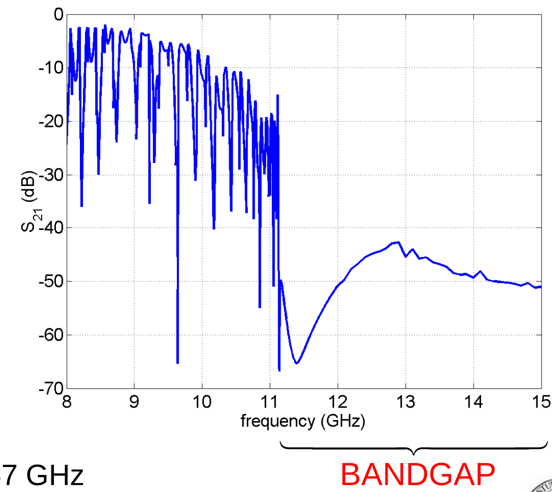

Stop band 11.14 – 15.57 GHz

Horizontal dipole – mutual coupling

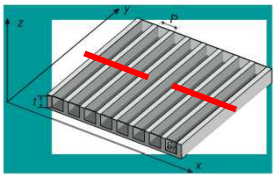

Dipoles:
- length: 10 mm
- height: 0.5 mm
- separation: 50 mm

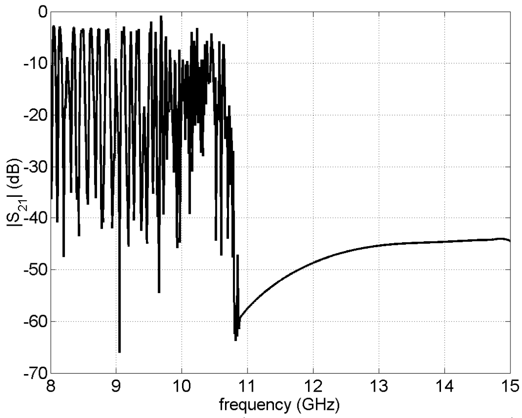

Stop band 11.0 – 22.0 GHz

BANDGAP

Horizontal dipole – radiation pattern

- Comparison of radiation pattern of vertical dipole over cylindrical EBG outside and inside band-gap (band-gap is 11.14 – 15.57 GHz)

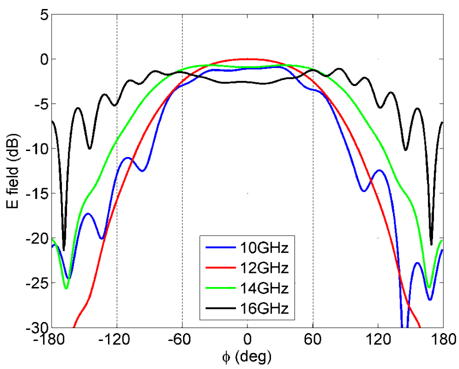

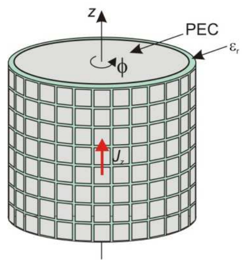

Horizontal dipole - input impedance

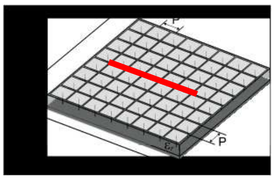

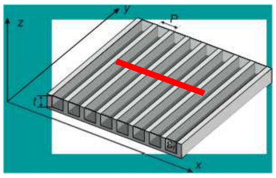

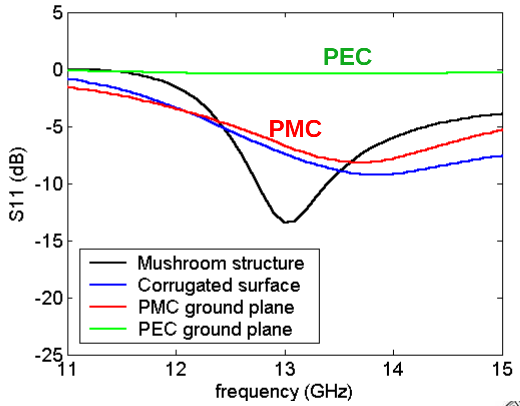

Dipole:

- length: 10 mm
- height: 0.5 mm

Horizontal dipole - input impedance

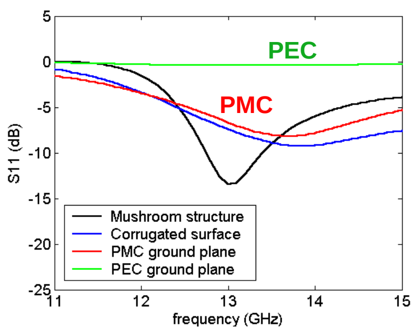

- It seems that dipole over PMC is not the best solution (even though it is only theoretical solution).
- Reason – mutual coupling between the dipole and the image.
- It seems that it is better if the periodic surface has freqency-dependend properties.

Reflection coefficient – normal incidence

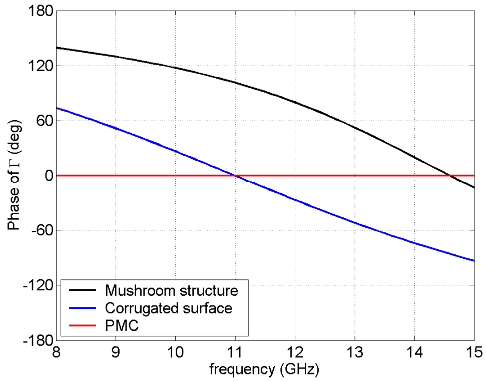

- It seems that it is better to select surface with phase of reflection coefficient around 60 degrees than “pure” PMC surface.

Outline

- Motivation
- Canonical surfaces, EBG surfaces, soft and hard surfaces
- **Applications**
- Modelling of EM surfaces
- G1DMULT and G2DMULT algorithms
- Story about cloaking

Reduction of sidelobes

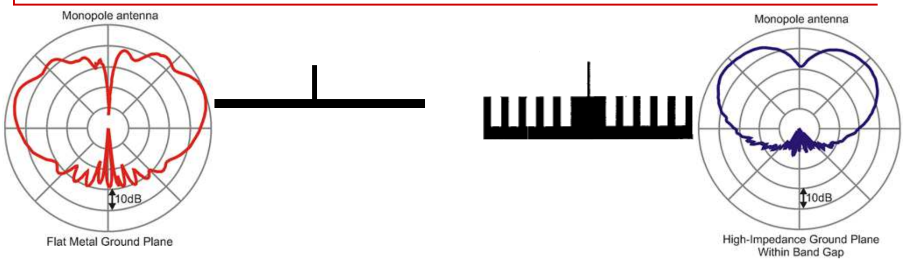

Bandwidth calculated from the shape of the radiation pattern

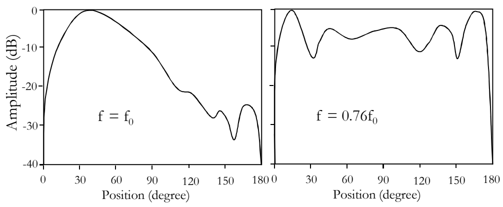

Bandwidth calculated from the back radiation efficiency

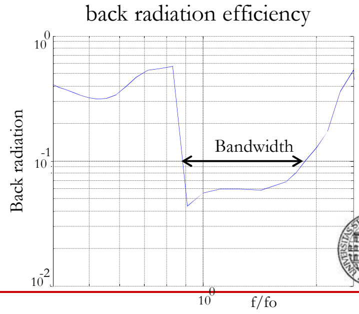

Picture: P.-S. Kildal

Reduction of sidelobes

- Ying, Kildal (1996):

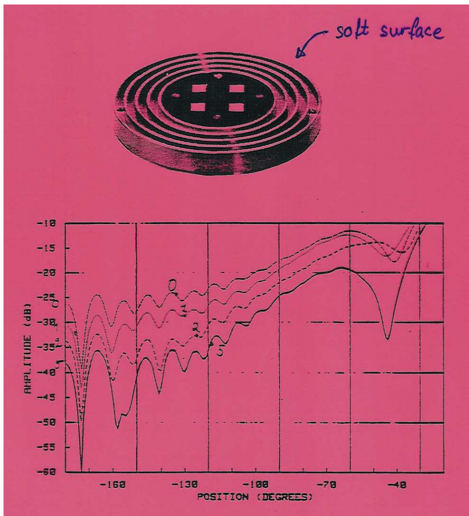

Corrugated horn

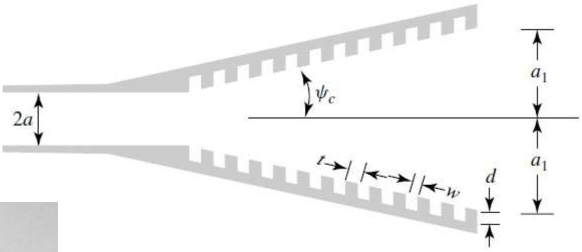

Pictures: C. A. Balanis
and March Microwave Systems, B.V.

Corrugated horn

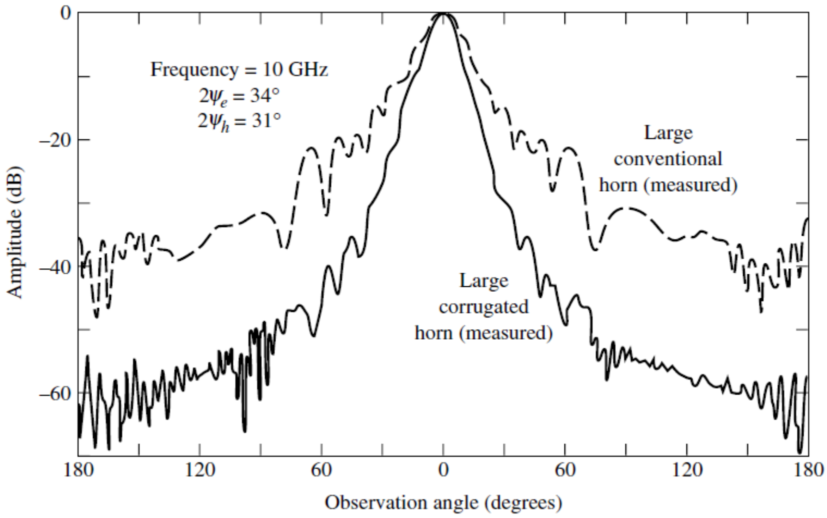

Picture: R. E. Laurie and L. Peters, Jr.,

Corrugated horn

- Broadband soft corrugated primary feed

  (Ying, A. Kishk and P-S. Kildal, 1995)

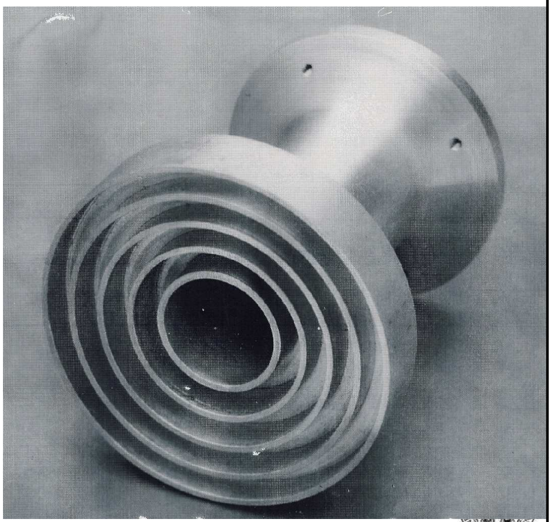

Corrugated horn

- Constant beamwidth over 0.9-1.7 GHz
- Aperture-field when used in Arecibo three-reflector system

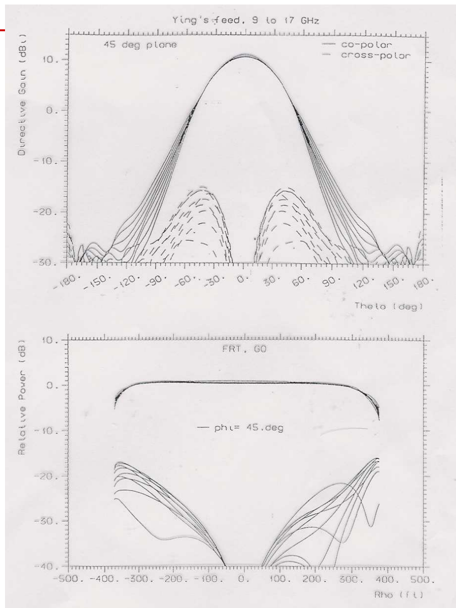

Hat feed antenna (Kildal)

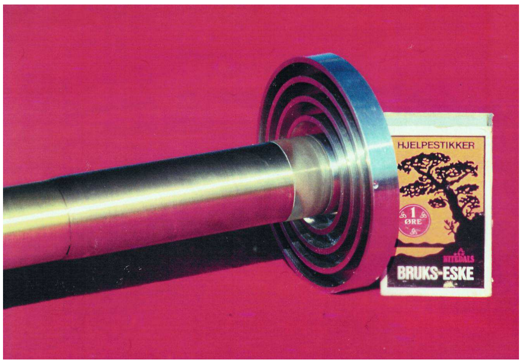

Around 1.000.000 hat-feed reflectors have been manufactured!

Low-profile antennas

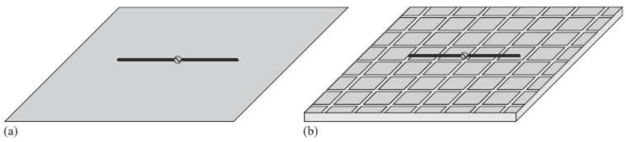

Fig. 6.1 Dipole antennas over (a) PEC or PMC ground plane and (b) EBG ground plane.

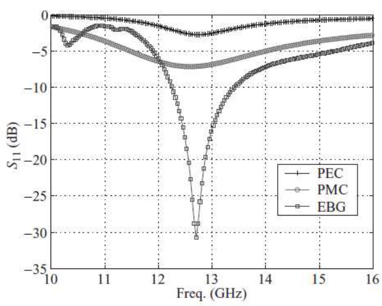

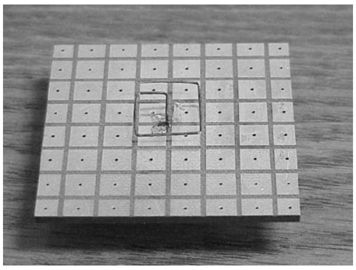

Fig. 6.2 Return loss comparison of dipole antennas over PEC, PMC, and EBG ground planes.

Picture: Yahya Rahmat Samii

Reduction of mutual coupling

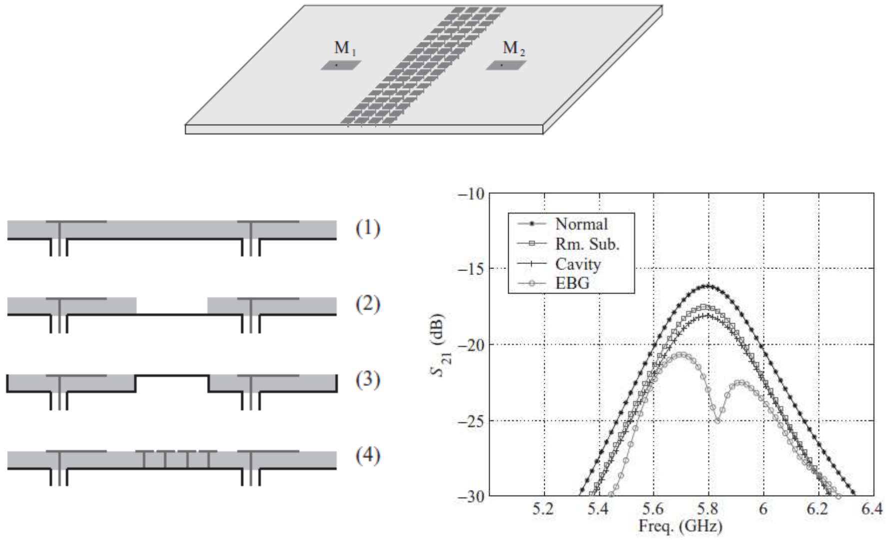

Picture: Yahya Rahmat Samii

Reduction of mutual coupling

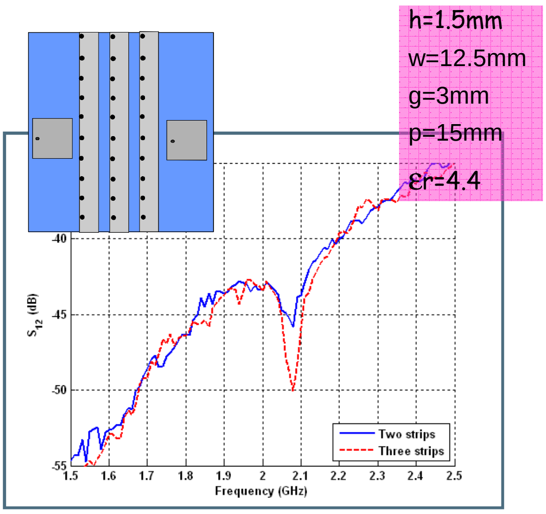

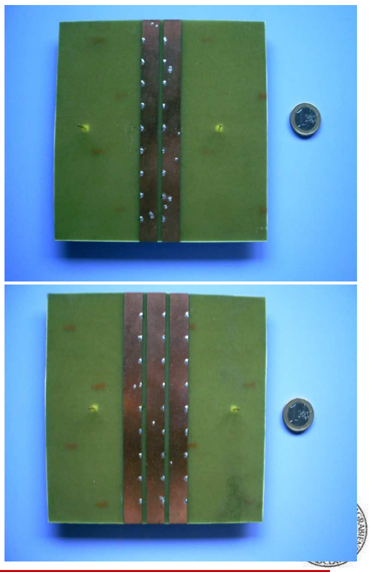

Picture: Eva Rajo-Iglesias, Oscar Quevedo-Teruel

Hard waveguides

- Linearly polarized hard waveguide using dielectric-loaded walls
- Rectangular waveguide:

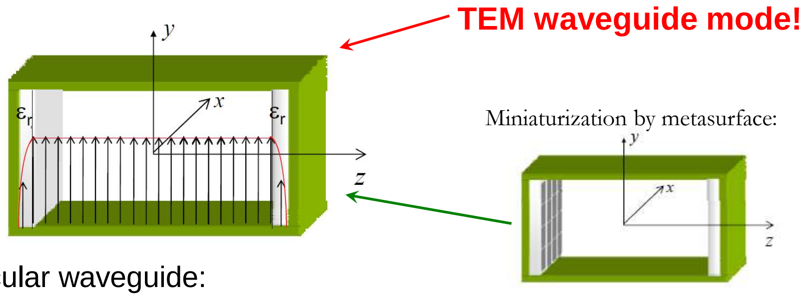

- Circular waveguide:

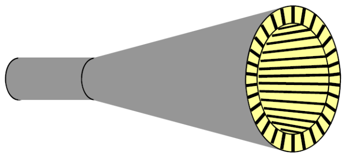

Picture: P.-S. Kildal

Hard waveguides

- Field distribution - rectangular waveguide:

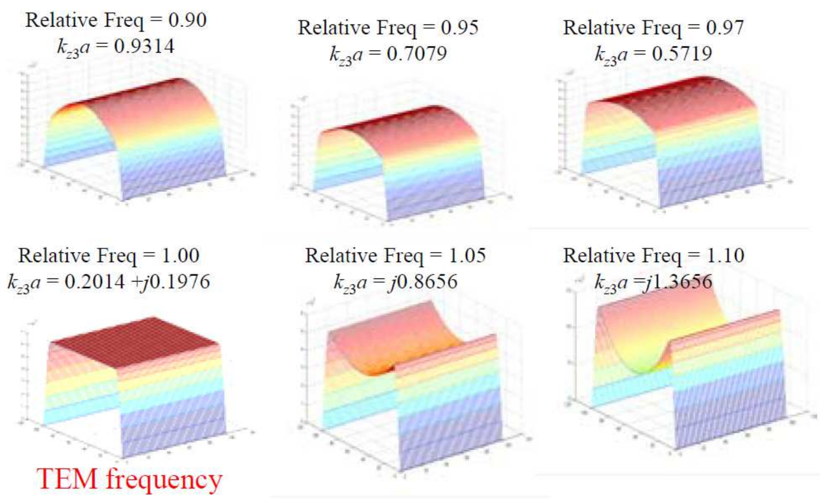

Picture: P.-S. Kildal

Hard waveguides

- Field distribution - circular waveguide:

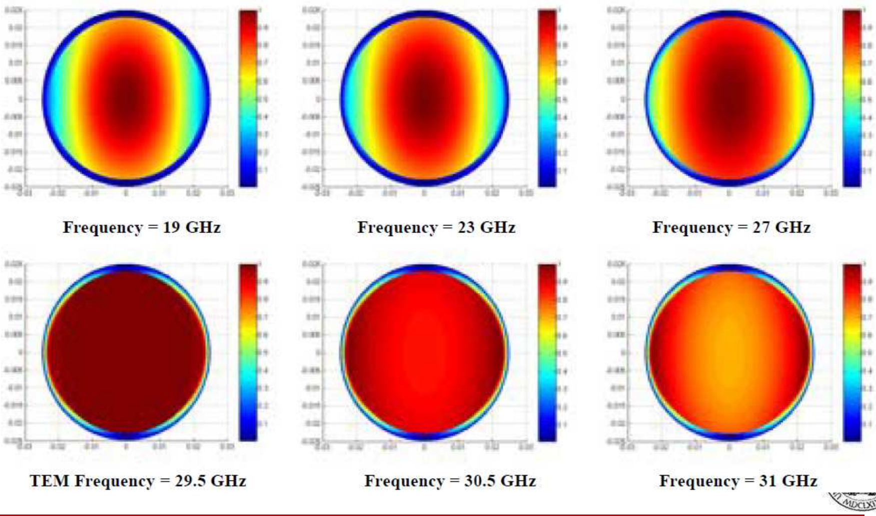

Picture: P.-S. Kildal

Hard waveguides

- Cluster feeds of a single-reflector multi-beam system.
- Uniform aperture distribution of feeds is advantageous.

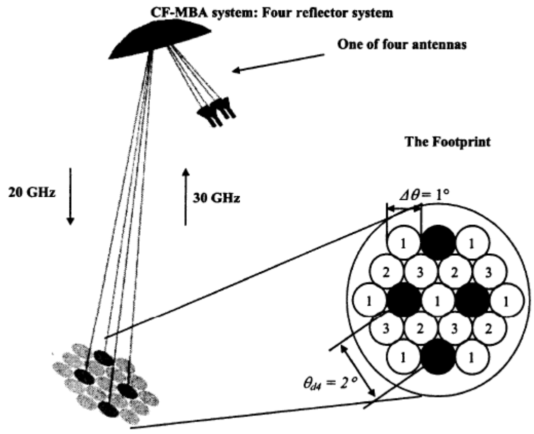

Hard waveguides

- Cluster feeds of a single-reflector multi-beam system.
- Uniform aperture distribution of feeds is advantageous.

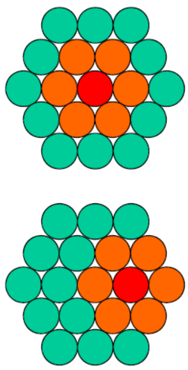

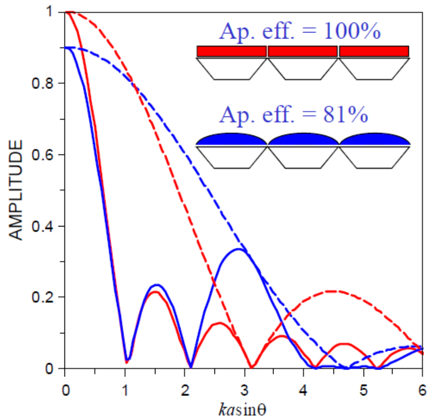

Picture: P.-S. Kildal

Hard struts

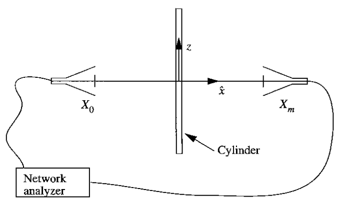

Picture: P.-S. Kildal

Hard struts

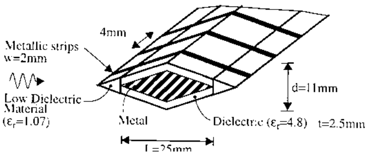

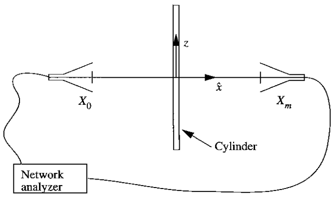

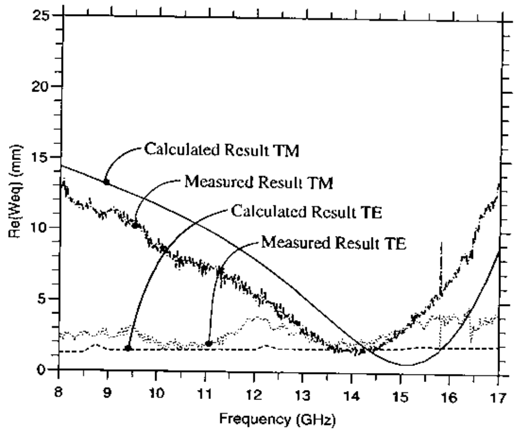

Picture: P.-S. Kildal

Hard struts

IEEE TRANSACTIONS ON ANTENNAS AND PROPAGATION, VOL. 44, NO. 11, NOVEMBER 1996 1509

Reduction of Forward Scattering from Cylindrical Objects using Hard Surfaces

Per-Simon Kildal, *Fellow, IEEE*, Ahmed A. Kishk, *Senior Member, IEEE*, and Audun Tengs

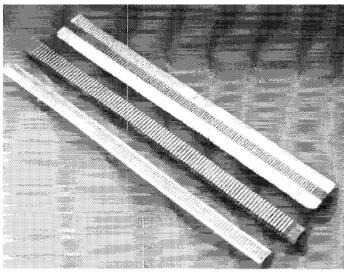

1150 IEEE TRANSACTIONS ON ANTENNAS AND PROPAGATION, VOL. 51, NO. 6, JUNE 2003

Analysis of Hard Surfaces of Cylindrical Structures of Arbitrarily Shaped Cross Section Using Asymptotic Boundary Conditions

Ahmed A. Kishk, *Fellow, IEEE*

Gap waveguides - Basic idea

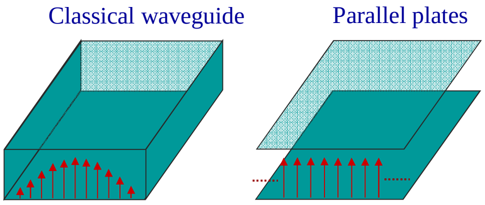

How to confine energy within a parallel-plate waveguide?

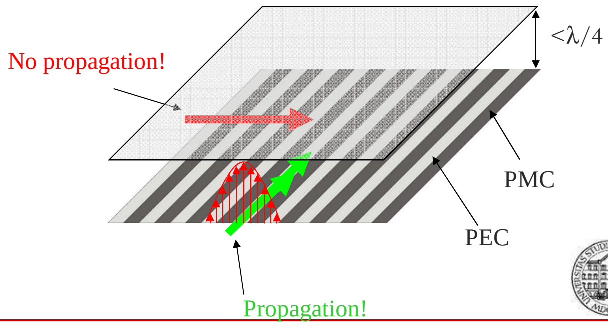

Gap waveguides - Motivation

- Applications above 30 GHz require new transmission lines
  - Radio astronomy, Earth observations, environmental surveillance, communication, imaging (medical and security)
- Problem: Hollow waveguides become expensive
  - Manufacturing in several pieces requires conducting joints
  - Too small hole diameter
- Problem: Microstrip-type lines are lossy
- Ground-braking solution: Gap waveguide
  - Only metal, no dielectric
  - No conducting joints needed
  - Low-cost milling, molding or etching

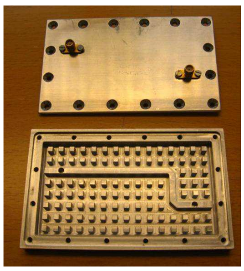

Structure developed at
Chalmers University of Technology

Fabrication challenges in millimeter-wave band

- ✓ Flatness is key to assure good contact between plates
- ✓ To assess good plate flatness is not an easy task

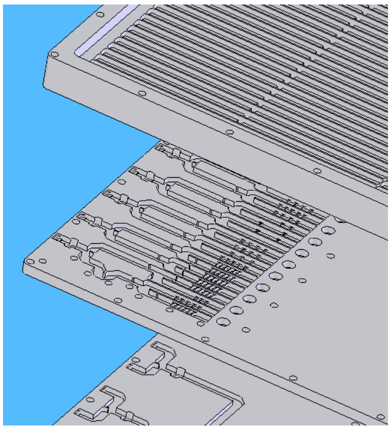

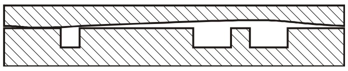

Picture: Alejandro Valero-Nogueira

Fabrication challenges in millimeter-wave band

- ✓ Many screws are needed to assure good contact, and not always successfully.

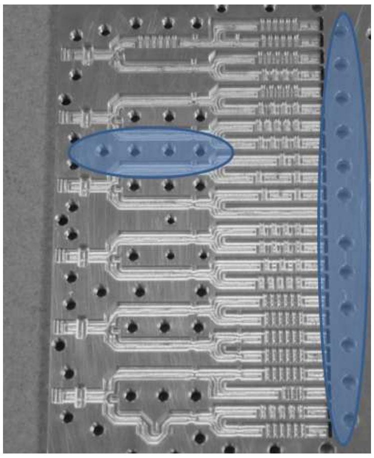

Feed network

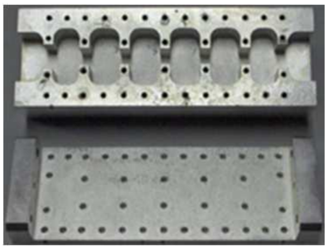

Filter

Picture: Alejandro Valero-Nogueira

Gap waveguides - 1D periodic structures

- Classical oversized waveguide:

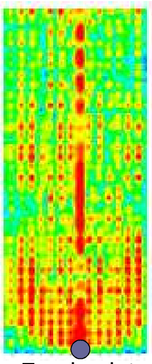

- Oversized waveguide with periodic texture (corrugations):

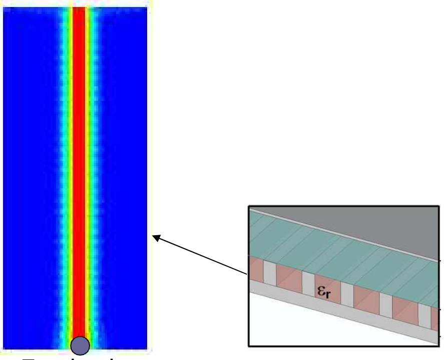

A. Valero-Nogueira, E. Alfonso, J.I. Herranz, and M. Baquero
Polytechnic University of Valencia, Spain

Gap waveguides - 1D periodic structures

- Slot array with steering beam possibility:

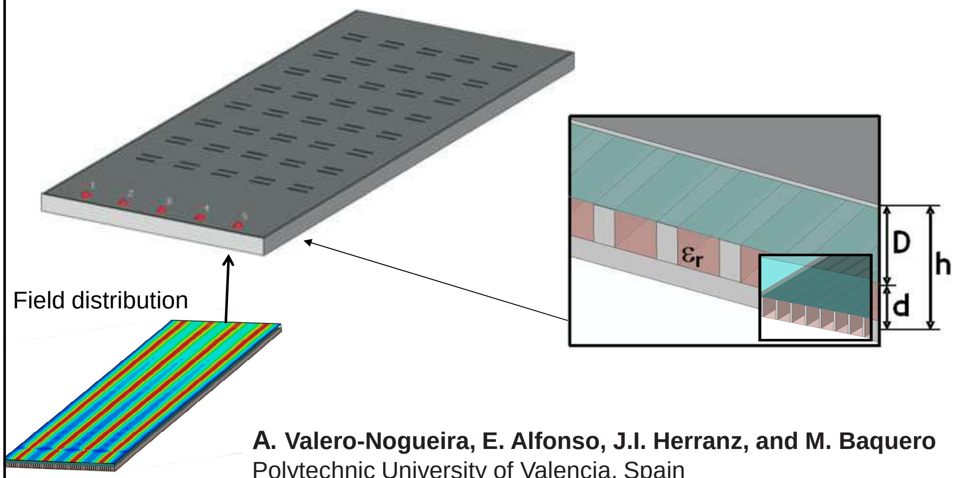

A. Valero-Nogueira, E. Alfonso, J.I. Herranz, and M. Baquero
Polytechnic University of Valencia, Spain

Gap waveguides
- 1D periodic structures

- Slot array with steering beam possibility:

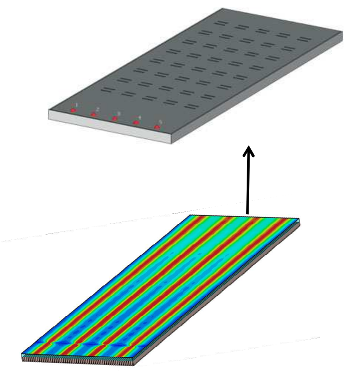

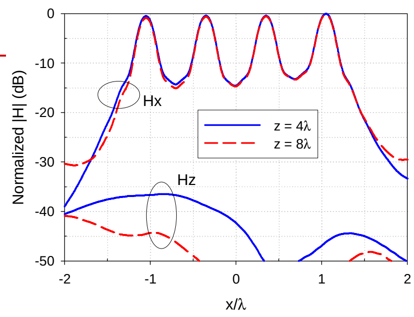

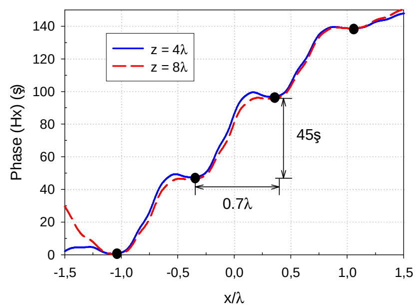

Gap waveguides

- Periodic structures can be divided into two types:
  - *1D periodic type (e.g. corrugations)*
  - *2D periodic type (e.g. bed of nails).*

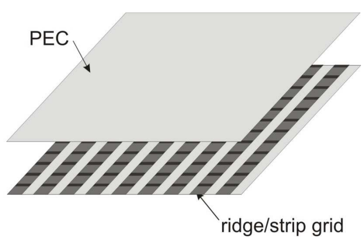

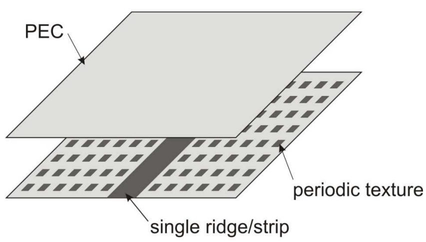

Gap waveguides - 2D periodic structures

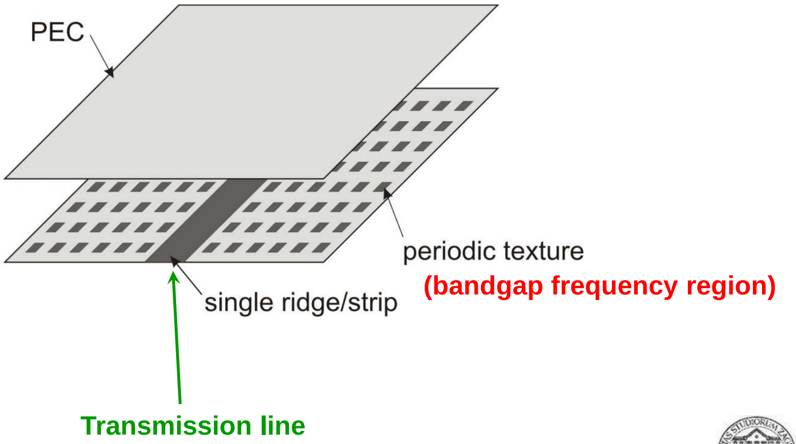

Parallel plate waveguide with 2D periodic structure

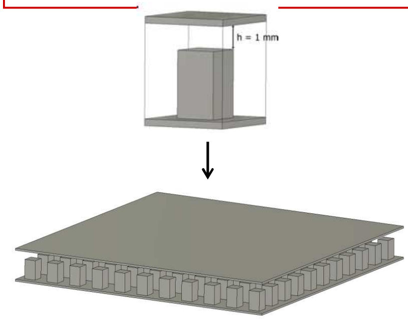

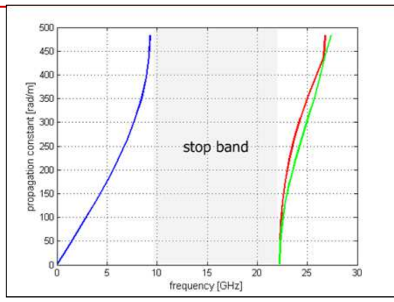

- **groove and ridge gap waveguide** – transmition line without lateral walls

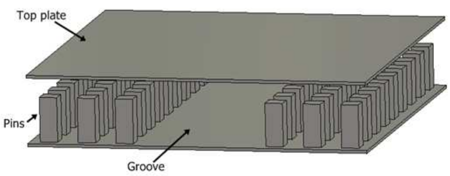

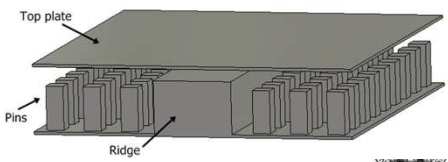

66

Field distribution inside ridge gap-waveguide

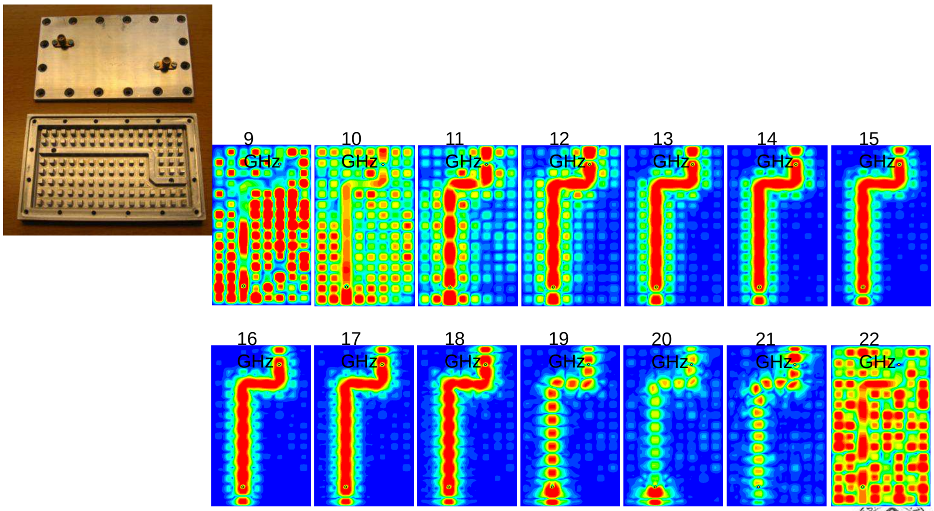

Structure developed at Chalmers University of Technology

Transverse plane field distributions (middle of gap)

Vertical field component

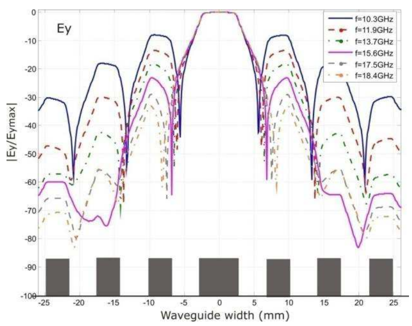

Horizontal field component

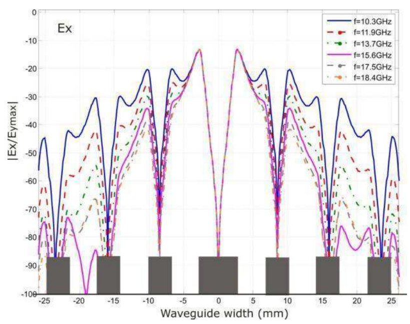

Structure developed at Chalmers University of Technology

Different components realized using gap-waveguide technology

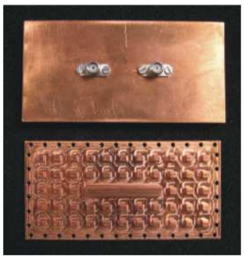

Resonator

Filters

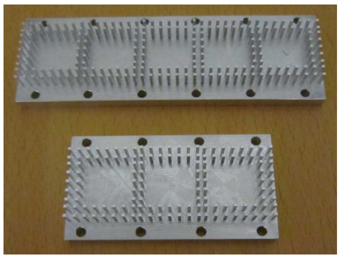

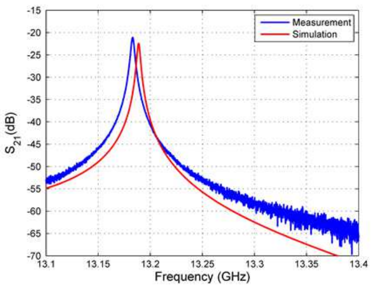

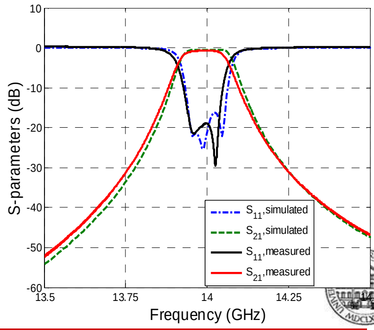

Structures developed at Chalmers University of Technology

Packaging: Measured S-parameters of bandpass filter

3rd order filter and lid of nails

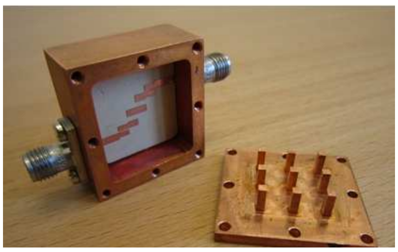

5th order filter and lids of nails

a) S21, 3rd order filter

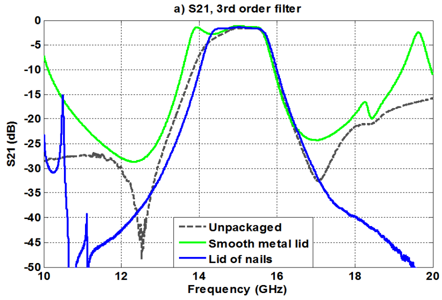

b) S11, 3rd order filter

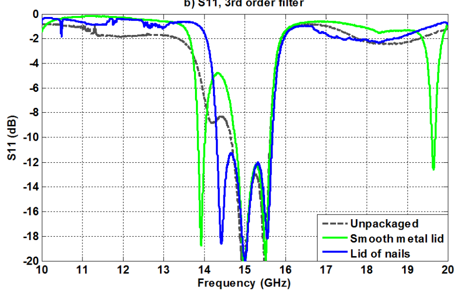

Structure developed at Chalmers University of Technology

Antennas in gap-waveguide technology

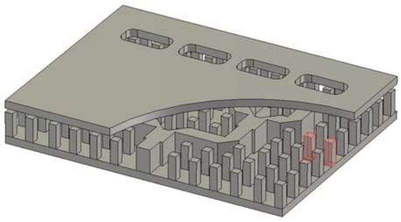

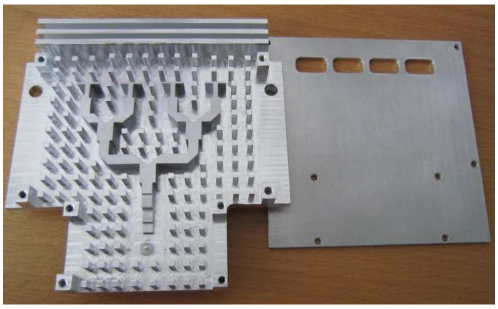

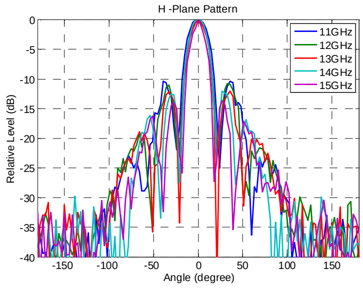

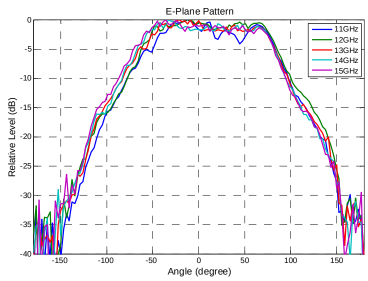

Structure developed at Chalmers University of Technology

Antennas in gap-waveguide technology

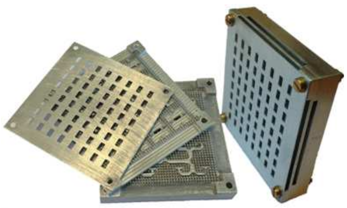

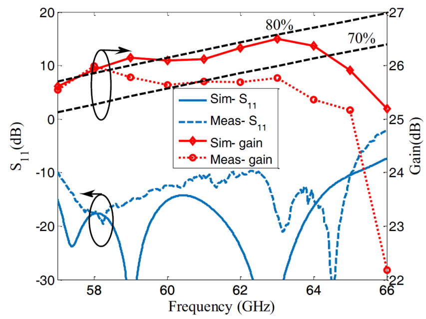

Pattern at 65 GHz

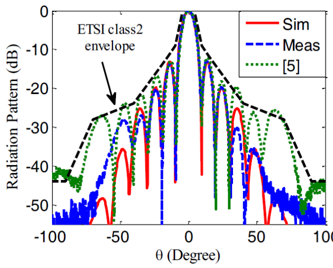

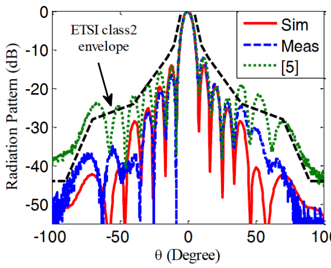

Structure developed at Chalmers University of Technology

Leaky Wave Antenna Integrated into Gap Waveguide Technology

Zvonimir Sipus[1], Mladen Vukomanovic[1], Jose-Luis Vazquez-Roy[2], Eva Rajo-Iglesias[2], and Oscar Quevedo-Teruel[3]

[1] University of Zagreb, Croatia
[2] University Carlos III of Madrid, Spain
[3] KTH Royal Institute of Technology, Sweden

Novel leaky wave antenna

- Antenna is based on the gap waveguide technology
- Requirements:
  - Simplicity
  - Only metal, no dielectric; no conducting joints needed
  - Suitable for applications above 30 GHz
  - Both the feeding structure and the antenna are realized in groove gap waveguide technology
  - Easiness of integration with traditional waveguide technology

Novel leaky wave antenna

- Concept: both the feeding structure and the antenna are realized in groove gap waveguide technology
- Based on the leak of electromagnetic fields at one side of the groove:

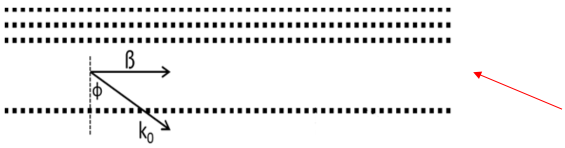

top view

- Amplitude and phase E-field distribution:

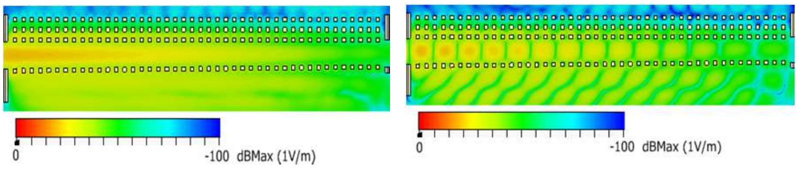

Novel leaky wave antenna

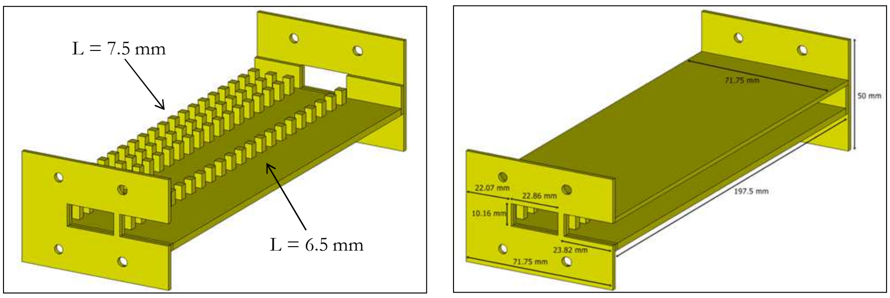

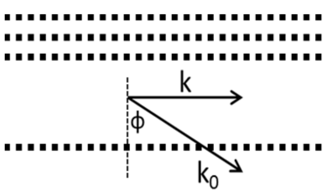

- Direction of the main beam:

$$\phi = \sin^{-1}(\beta / k_0)$$

Novel leaky wave antenna

1st antenna design

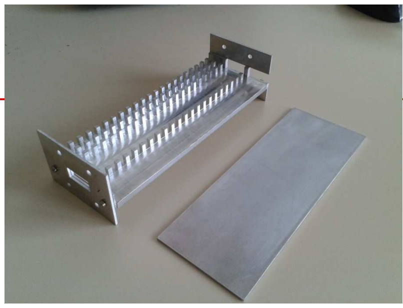

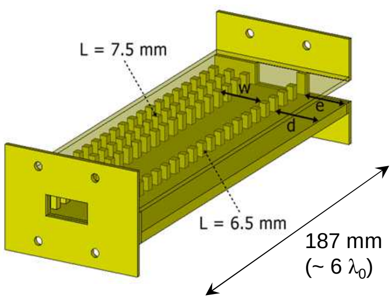

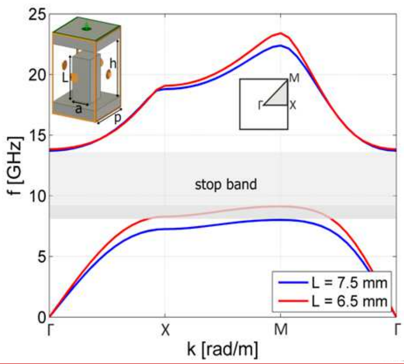

Gap waveguide leaky wave antenna

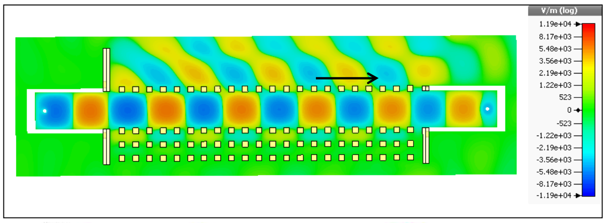

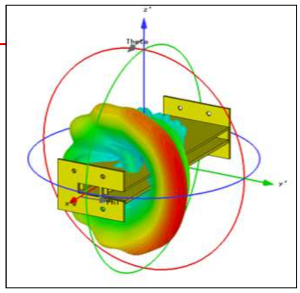

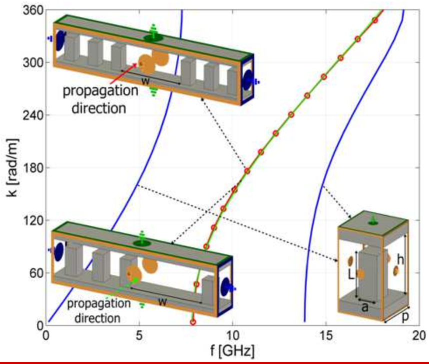

- **Gain: 12.81 dB**
- Main lobe dir.: 49.0 deg
- 3 dB beam width: 10.4 deg
- Side lobe level: -10.37 dB

Gap waveguide leaky wave antenna

- Measured radiation pattern:

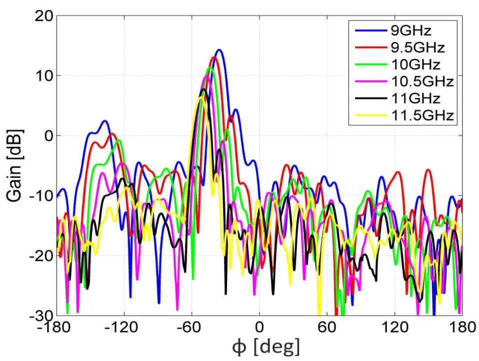

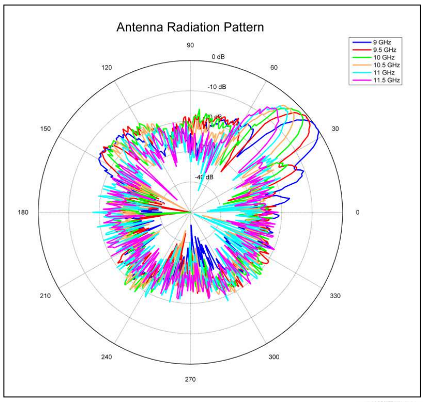

Gap waveguide leaky wave antenna

Characterization of LWA:

- Radiation pattern
- Gain
- Side-lobe level
- S-parameters

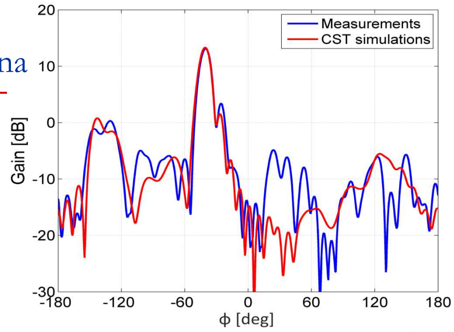

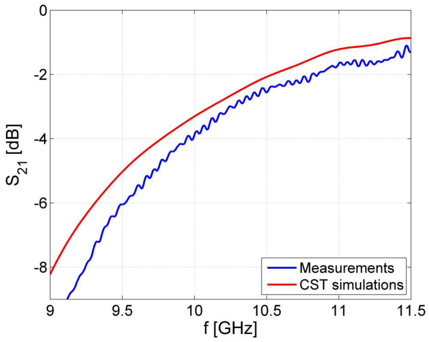

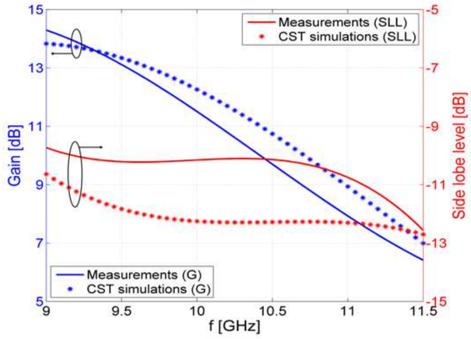

Novel leaky wave antenna

2nd antenna design

Gap waveguide leaky wave antenna – 2nd prototype

L_1 = 7.5 mm
L_2 = 6.5 mm
W_1 = 22 mm
W_2 = 18.8 mm

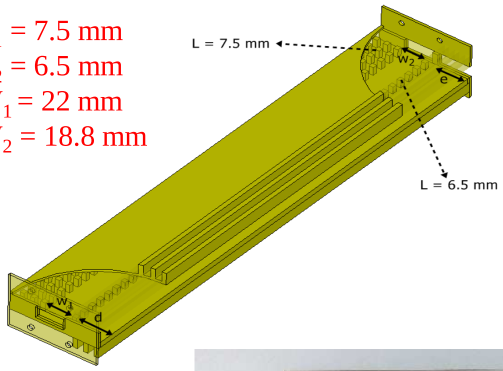

Design steps:

- Different heights of pins
- Width of the groove waveguide is gradually changed
- Corrugations on the top and bottom plate to reduce back-radiation

Design of gap waveguide leaky wave antenna

- Design is based on tailoring complex propagation constant:

$$\gamma = \alpha + j\beta$$

- Phase constant:

$$\beta \approx k_0 \sqrt{1-\left(\lambda/2w_{eff}\right)^2}$$

- Attenuation (radiation) constant:

$$\alpha \sim \left[\lambda \Big/ \sqrt{1-\left(\lambda/2w_{eff}\right)^2}\right]^4$$

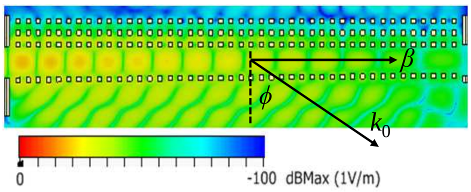

Goal: to radiate 90% of the incoming power

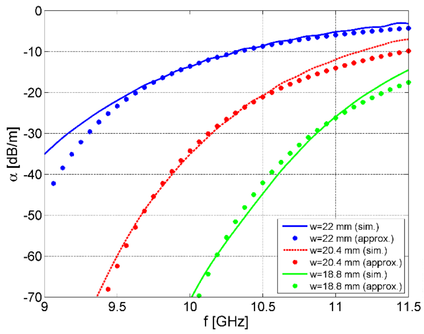

Design of gap waveguide leaky wave antenna

- Problem of strong back-side radiation:

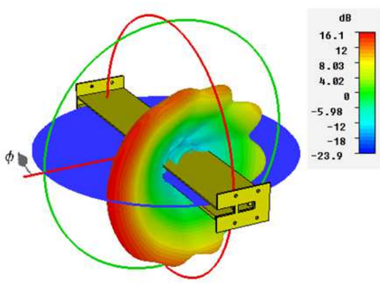

- Solution - corrugations:

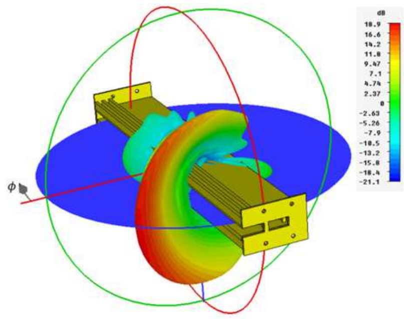

Leaky wave antenna – measured results

Radiation pattern

- Direction of the main beam:

$$\phi \approx \sin^{-1}(\beta/k_0)$$

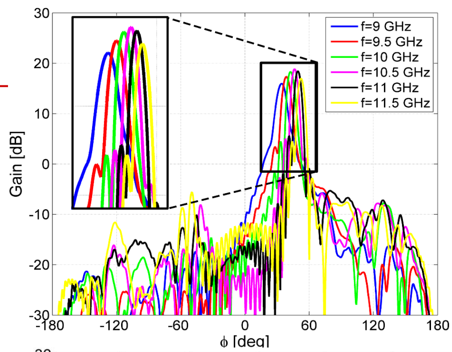

- Comparison of calculated results and measurements at 10 GHz:

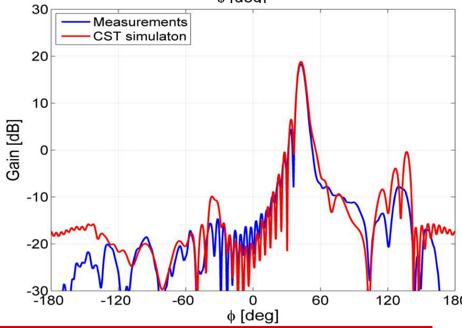

Leaky wave antenna – measured results

Measurements and simulations:

- S-parameters
- gain (G) – higer than 16 dB
- SLL - lower than -10 dB

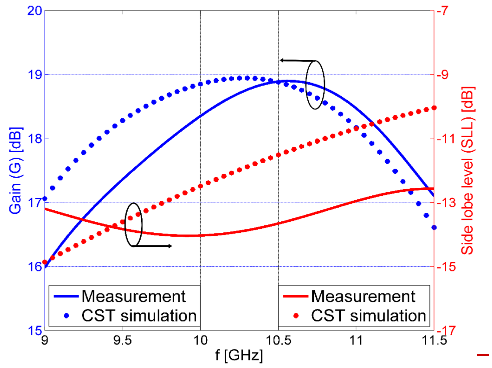

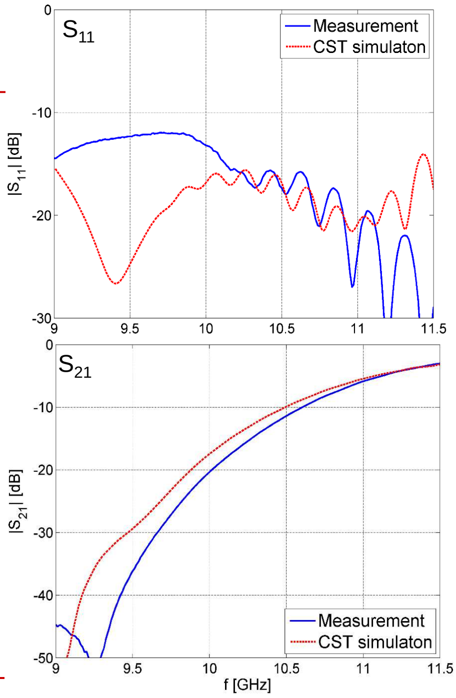

Design of gap-waveguide components

- Natural way of designing devices:

Concept development

↓

Device development

↓

Practical realization

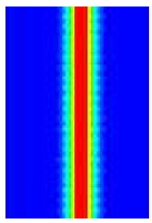

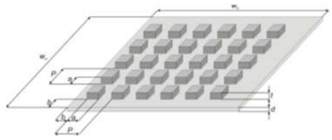

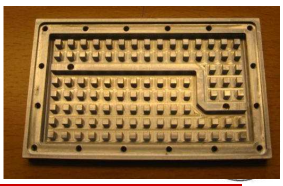

Outline

- Motivation
- Canonical surfaces, EBG surfaces, soft and hard surfaces
- Applications
- **Modelling of EM surfaces**
- G1DMULT and G2DMULT algorithms
- Story about cloaking

Theoretical background

The analysis and desing method is based on:

- Spectral-domain method (plane wave expansion in the planar case)
- Asymptotic boundary conditions for modelling the metal pattern layers
- Equivalence principle for analyzing multilayer and multiregion structures

Plane wave expansion

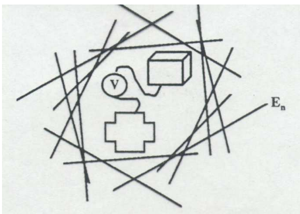

- In a homogeneous media, all finite sources may be represented by a set of plane waves with various propagation directions, amplitudes and phases.

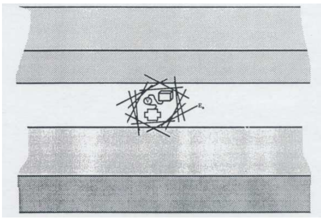

- In multilayer structures, for each plane wave excited by the source we need to solve one-dimensional (1D) problem.

Plane wave representation – general multilayer problem

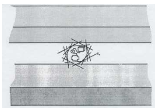

- In the *i*th layer the EM field can be represented as (sum of forward and backward propagating waves) :

$$\mathbf{E}(x,y,z)=\mathbf{E}(z)\cdot e^{-jk_x^i x}e^{-jk_y^i y} \qquad \mathbf{H}(x,y,z)=\mathbf{H}(z)\cdot e^{-jk_x^i x}e^{-jk_y^i y}$$

- At each boundary the tangential components of the E- and H-field are continuous

$$e^{-jk_x^i x}e^{-jk_y^i y}=e^{-jk_x^{i+1} x}e^{-jk_y^{i+1} y} \qquad i=1,\ldots,N_{boundary}$$

- Consequently, variation of the total field in *x*- and *y*-directions:

$$e^{-jk_x x}e^{-jk_y y}$$

- For each plane wave excited by the source we need to solve one-dimensional (1D) problem.

Mathematical background of plane wave representation

- Definition of two-dimensional Fourier transformation in the directions where the structure is homogeneous:

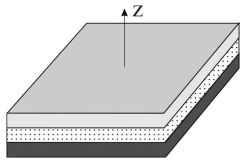

$$\tilde{\mathbf{E}}(k_x, k_y, z) = \int_{-\infty}^{\infty}\int_{-\infty}^{\infty} \mathbf{E}(x, y, z) e^{jk_x x} e^{jk_y y}\, dxdy$$

- Useful properties of Fourier transformation:

$$\frac{\partial f}{\partial x} \Leftrightarrow -jk_x \tilde{f}, \qquad \frac{\partial f}{\partial y} \Leftrightarrow -jk_y \tilde{f}, \qquad f * g \Leftrightarrow \tilde{f} \cdot \tilde{g}$$

- The form of Helmholtz differential equation $\nabla^2 E_z + k^2 E_z = 0$ after performing the Fourier transformation:

$$\left(\frac{\partial^2}{\partial z^2} + \underbrace{k^2 - k_x^2 - k_y^2}_{k_z^2}\right)\tilde{E}_z(k_x, k_y, z) = 0$$

Mathematical background of plane wave representation

- The solution of modified Helmholtz differential equation is:

$$\tilde{E}_z(k_x, k_y, z) = C_1 e^{-jk_z z} + C_2 e^{jk_z z},$$

$$\tilde{H}_z(k_x, k_y, z) = C_3 e^{-jk_z z} + C_4 e^{jk_z z},$$

$$k_z^2 = k^2 - k_x^2 - k_y^2$$

- In other words, for each k_x and k_y we need to determine four constants C_1, C_2, C_3 and C_4. They are determined by fulfilling the boundary conditions (1D problem).
- Another form of the solution:

$$\tilde{E}_z(k_x, k_y, z) = D_1 \cos(k_z z) + D_2 \sin(k_z z),$$

$$\tilde{H}_z(k_x, k_y, z) = D_3 \cos(k_z z) + D_4 \sin(k_z z).$$

Mathematical background of plane wave representation

- Definition of inverse Fourier transformation

$$\mathbf{E}(x,y,z)=\frac{1}{4\pi^2}\int_{-\infty}^{\infty}\int_{-\infty}^{\infty}\tilde{\mathbf{E}}(k_x,k_y,z)\,e^{-jk_x x}e^{-jk_y y}\,dk_x dk_y$$

$$\cong\sum_m\sum_n\frac{1}{4\pi^2}\tilde{\mathbf{E}}(k_x,k_y,z)\Delta k_x\Delta k_y\;e^{-jk_x x}e^{-jk_y y}$$

$$=\sum_m\sum_n\left[C_{i,1}e^{-jk_z^i z}+C_{i,2}e^{jk_z^i z}\right]e^{-jk_x x}e^{-jk_y y}$$

$$k_z^i=\sqrt{k_0^2\varepsilon_{i,r}-k_x^2-k_y^2}$$

- The inverse Fourier transformation has a form of a sum of plane waves.
- Therefore, the Fourier transformation represents the tool for obtaining the plane wave representation of the EM fields.

Plane wave expansion

- Physical picture of the spectral-domain Green's function of a point source in homogeneous space:

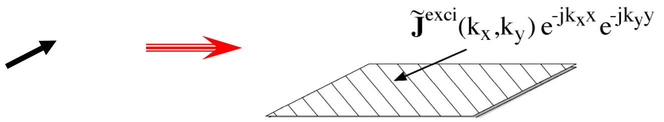

space domain spectral domain

- Radiation of the current sheet:

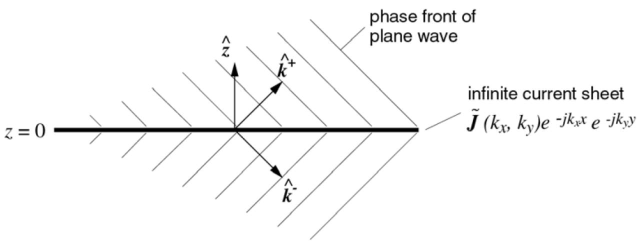

Plane wave expansion

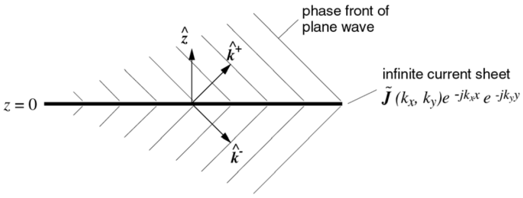

- E- and H- fields from electric current sheet

$$\tilde{\mathbf{E}} = \begin{cases} -\dfrac{k}{2k_z}\left[\eta\tilde{\mathbf{J}} - \left(\eta\tilde{\mathbf{J}}\cdot\hat{k}^+\right)\hat{k}^+\right]e^{-jk\hat{k}^+\cdot\mathbf{r}} & z > 0 \\ -\dfrac{k}{2k_z}\left[\eta\tilde{\mathbf{J}} - \left(\eta\tilde{\mathbf{J}}\cdot\hat{k}^-\right)\hat{k}^-\right]e^{+jk\hat{k}^-\cdot\mathbf{r}} & z < 0 \end{cases}$$

$$\eta\tilde{\mathbf{H}} = \begin{cases} \dfrac{k}{2k_z}\left[\eta\tilde{\mathbf{J}}\times\hat{k}^+\right]e^{-jk\hat{k}^+\cdot\mathbf{r}} & z > 0 \\ \dfrac{k}{2k_z}\left[\eta\tilde{\mathbf{J}}\times\hat{k}^-\right]e^{+jk\hat{k}^-\cdot\mathbf{r}} & z < 0 \end{cases}$$

where $\hat{k}^+ = (k_x\hat{x} + k_y\hat{y} + k_z\hat{z})/k$ and $\hat{k}^- = (k_x\hat{x} + k_y\hat{y} - k_z\hat{z})/k$.

Summary of spectral domain method

- Two-dimensional Fourier transformation is applied in directions where the structure is homogeneous.
- In these two directions each spectral component of EM field has the same variation as the source.
- Therefore, three-dimensional problem is transformed in spectrum of one-dimensional problems.

Asymptotic boundary conditions
Ideal PEC/PMC model

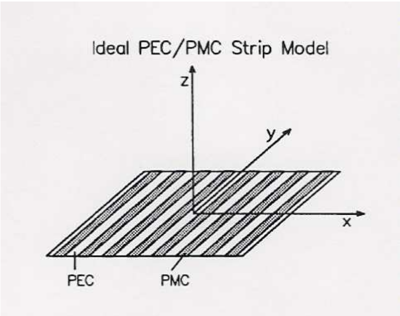

- If the PEC/PMC strips are parallel to the y axis, the boundary conditions at the surface are

$$E_y^{air} = 0, \qquad H_y^{air} = 0.$$

- These boundary conditions are valid in an asymptotic way, when the width and the periodicity of the strips approach zero.

Parallel plate waveguide with PEC/PMC strips

- We would like to derive the Green's function for the H-field of the parallel plate waveguide with one wall containing PEC/PMC strips.
- The source is z-directed short dipole.

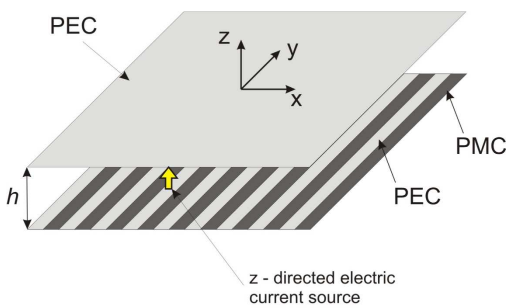

Parallel plate waveguide with PEC/PMC strips

- E_z and H_z components of the EM field has the form (we need to determine constants A, B, C and D):

$$\tilde{E}_z(k_x,k_y,z) = A\cos(k_z z) + B\sin(k_z z),$$
$$\tilde{H}_z(k_x,k_y,z) = C\cos(k_z z) + D\sin(k_z z).$$

- The boundary conditions:

$$\tilde{E}_y = 0, \qquad \tilde{H}_y = 0 \qquad\qquad \text{for } z = 0$$
$$\tilde{E}_x = \tilde{M}_y, \qquad \tilde{E}_y = -\tilde{M}_x \qquad\qquad \text{for } z = h$$

- The replacement magnetic currents are:

$$\tilde{M}_x = \frac{k_y}{k_0/\eta_0}\tilde{J}_z, \qquad \tilde{M}_y = -\frac{k_x}{k_0/\eta_0}\tilde{J}_z$$

Parallel plate waveguide with corrugated surface

Dispersion diagram for the parallel-plate waveguide with corrugations:

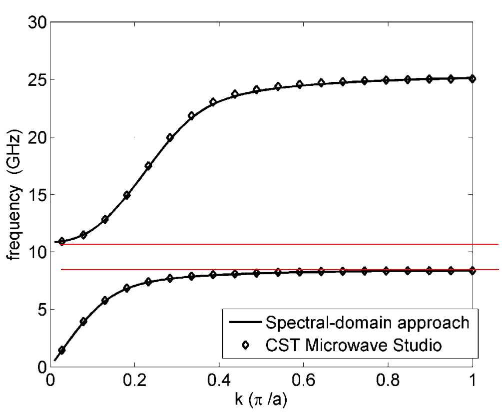

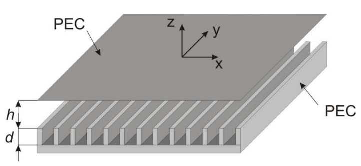

Cut-off observed between 8.66 GHz and 10.85 GHz

Parallel plate waveguide with corrugated surface

- H_x component at the point ($x = 0$, $y = 4.5\ \lambda_0$, $z = h$) and H_y component at the point ($x = 1.0\ \lambda_0$, $y = 0$, $z = h$), as a function of frequency.

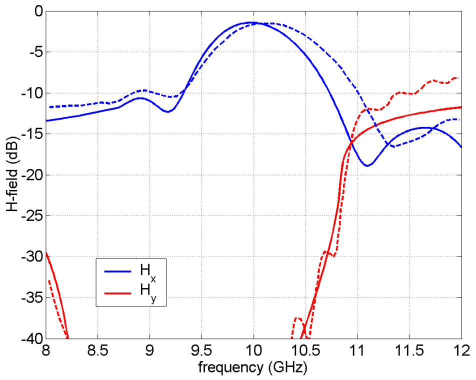

— Asymptotic boundary conditions

---- CST; calculated by Esperanza Alfonso

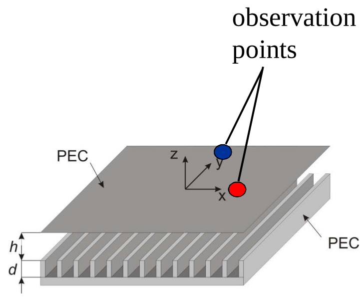

$f_0 = 10$ GHz
$h = 3.5$ mm
$d = 4.33$ mm
$\varepsilon_r = 4.0$

Parallel plate waveguide with corrugated surface

- H_x component of the near magnetic field in the plane defined by $z = h$, $y = 1.0\ \lambda_0$ and $y = 5.0\ \lambda_0$.

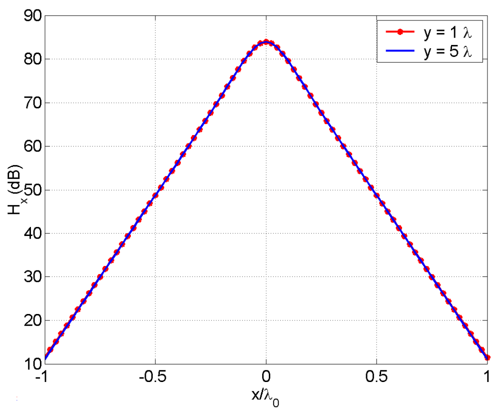

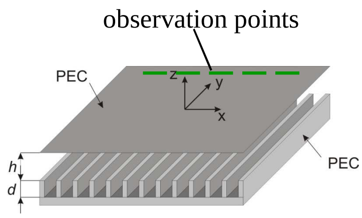

$f = 10$ GHz
$h = 3.5$ mm
$d = 4.33$ mm
$\varepsilon_r = 4.0$

Concept: Parallel plate waveguide with bed-of-nails

- Bed-of-nails acts like a two-dimensional corrugated surface.
- The analysis is based on spectral surface impedance.

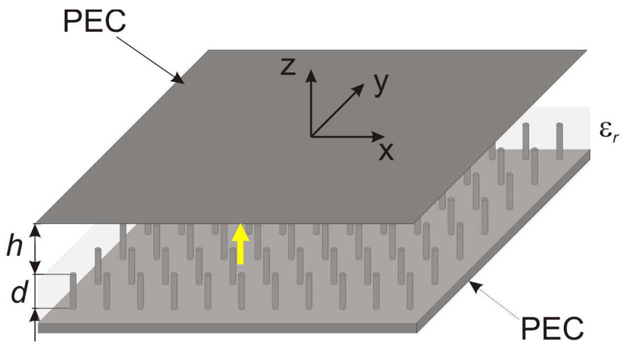

Parallel plate waveguide with bed-of-nails

- The wire medium is modelled as a infinitely long thin metallic rods:

$$\overline{\overline{\varepsilon}} = \varepsilon_0 \varepsilon_h (\hat{x}\hat{x} + \hat{y}\hat{y} + \varepsilon_{zz}(\omega, k_z)\hat{z}\hat{z})$$

$$\varepsilon_{zz}(\omega, k_z) = 1 - \frac{k_p^2}{k_0^2 \varepsilon_h - k_z^2}$$

$$k_p^2 = \frac{1}{a^2}\left[2\pi \Big/ \left(\ln\left(\frac{a}{2\pi b}\right) + 0.5275\right)\right]$$

- Three types of modes are propagating inside bed of nails:
  - TE mode: $\xi^2 = k^2 \varepsilon_h$
  - TEM mode: $\xi^2 = k_z^2$
  - TM mode: $\xi^2 = k_p^2 + k^2 \varepsilon_h$

Parallel plate waveguide with bed-of-nails

- Three types of modes are propagating inside bed of nails:
  - TE mode: $\xi^2 = k^2 \varepsilon_h$
  - TEM mode: $\xi^2 = k_z^2$
  - TM mode: $\xi^2 = k_p^2 + k^2 \varepsilon_h$

TE mode   TM mode

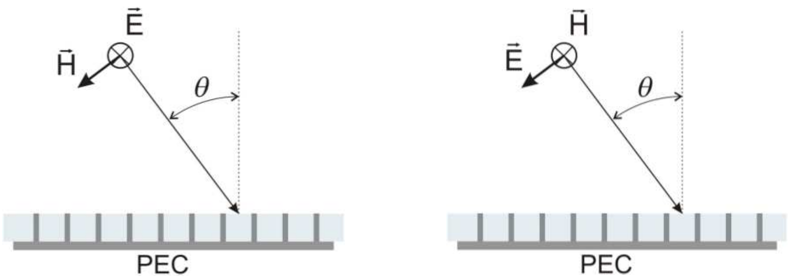

Parallel plate waveguide with bed-of-nails

- Spectral surface admittance is determined from the value of reflection coefficient.
- TM case:

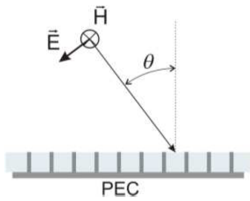

$$\tilde{Y}_{xy}^{TM} = \tilde{Y}_{yx}^{TM} = \frac{k_0}{\eta_0 k_z} \cdot \frac{\Gamma^{TM} + 1}{\Gamma^{TM} - 1}$$

$$\Gamma^{TM} = -\frac{k_{die} k_p^2 \tan(k_{die} d) - \beta^2 \gamma_{TM} \tanh(\gamma_{TM} d) + \varepsilon \gamma_0 (k_p^2 + \beta^2)}{k_{die} k_p^2 \tan(k_{die} d) - \beta^2 \gamma_{TM} \tanh(\gamma_{TM} d) - \varepsilon \gamma_0 (k_p^2 + \beta^2)}$$

$$\beta^2 = k_x^2 + k_y^2 \qquad \gamma_0 = \sqrt{\beta^2 - k_0^2} \qquad \gamma_{TM} = \sqrt{k_p^2 + \beta^2 - k_{die}^2}$$

$$k_p^2 = \frac{1}{a^2}\left[2\pi \Big/ \left(\ln\left(\frac{a}{2\pi b}\right) + 0.5275\right)\right]$$

- Details: M.G. Silveirinha *et all.*, IEEE AP Trans., Feb. 2008.

Mushroom structure

TE case:

- The pins are “invisible” for TE waves, i.e. the reflection coefficient is equal to the reflection coefficient of grounded delectric slab.

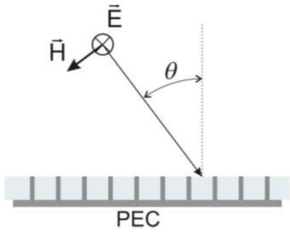

$$\tilde{Y}_{xy}^{TE} = \tilde{Y}_{yx}^{TE} = \frac{k_z}{\eta_0 k_0} \cdot \frac{\Gamma^{TE} + 1}{\Gamma^{TE} - 1}$$

$$\Gamma^{TE} = -\frac{\sqrt{k_{die}^2 - \beta^2} - j\sqrt{k_0^2 - \beta^2}\tan\left(d\sqrt{k_{die}^2 - \beta^2}\right)}{\sqrt{k_{die}^2 - \beta^2} + j\sqrt{k_0^2 - \beta^2}\tan\left(d\sqrt{k_{die}^2 - \beta^2}\right)}$$

Parallel plate waveguide with bed-of-nails

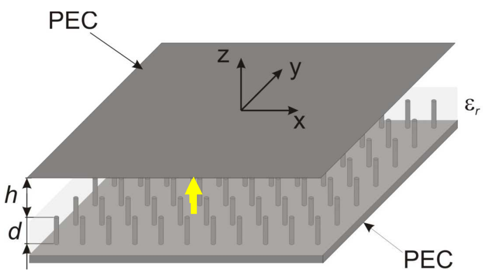

- Surface waves are determined by the characteristic equation:

$$D_{sw} = -\tilde{Y}_{yx}\left(k_0^2 - k_x^2\right) - \tilde{Y}_{xy}\left(k_0^2 - k_y^2\right)$$
$$+ jk_0 k_z\left[\eta_0 \tan(k_z h)\tilde{Y}_{xy}\tilde{Y}_{yx} - \frac{1}{\eta_0}\cot(k_z h)\right]$$

Parallel plate waveguide with bed-of-nails

- Dispersion diagram for the parallel-plate waveguide with bed-of-nails and additional dielectric layer :

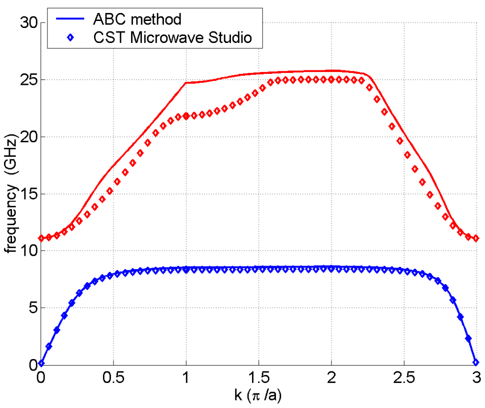

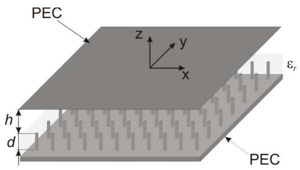

h = 3.5 mm
d = 4.33 mm
ε_r = 4.0

Band-gap:
8.6 – 11.1 GHz

Experimental prototype

- Dispersion diagram for the prototype gap-waveguide with bed-of-nails:

w_a	w_b	P (mm)	a (mm)	b (mm)	t (mm)	d (mm)
150	150	7.5	3.5	3.75	10	10

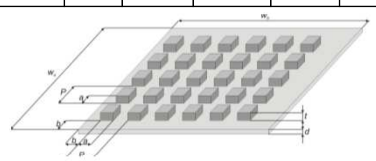

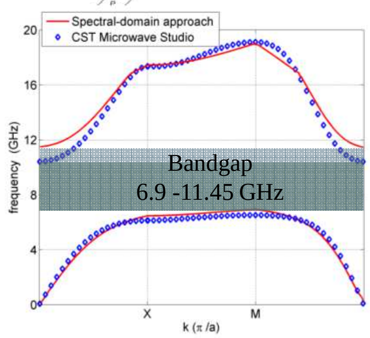

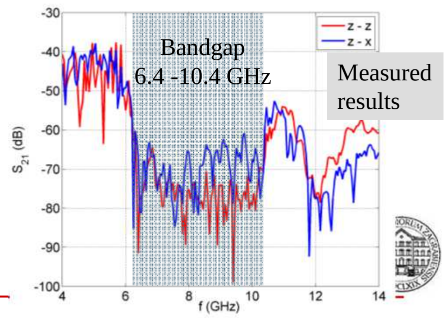

Parallel plate waveguide with bed-of-nails and a ridge

- Propagation constant of the fundamental mode

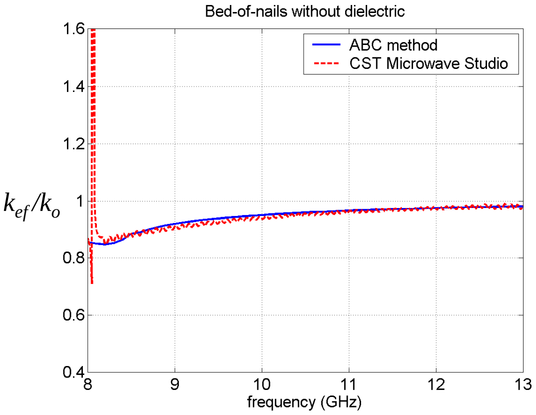

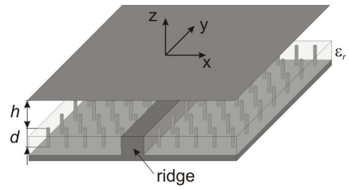

h = 3.5 mm
d = 8.66 mm
ε_r = 1.0

Parallel plate waveguide with bed-of-nails and a ridge

- Field distribution above the ridge and above the bed-of-nails:

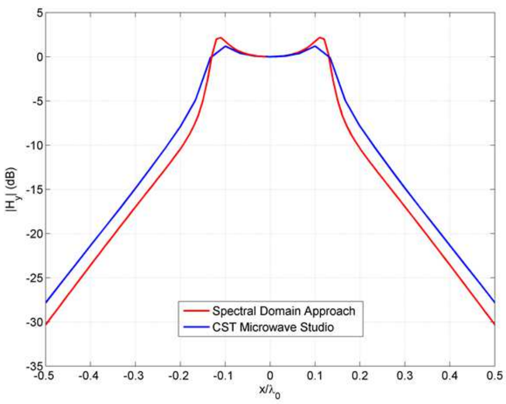

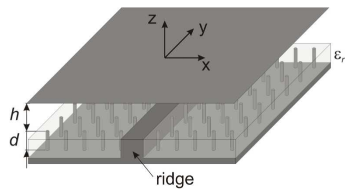

$y = 3\lambda_0$

- field computed 0.5 mm above the ridge

h = 3.5 mm
d = 4.33 mm
ε_r = 4.0

Parallel plate waveguide with bed-of-nails and a ridge

Characteristic impedance of the waveguide:

$$Z_0 = 2P/I^2$$

$$P = \int_0^{h_w}\int_{-\infty}^{\infty}(E_z H_x^* - E_x H_z^*)\,dS = \frac{1}{2\pi}\int_0^{h_w}\int_{-\infty}^{\infty}(\tilde{E}_z \tilde{H}_x^* - \tilde{E}_x \tilde{H}_z^*)\,dk_x\,dz$$

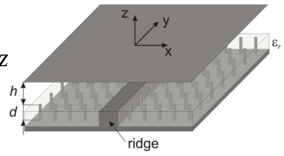

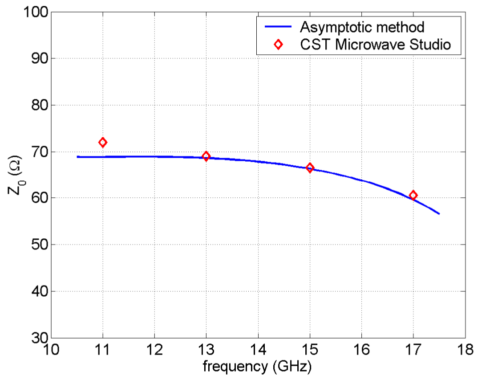

h = 1.0 mm
d = 7.5 mm
ε_r = 1.0
a = 2 mm
W = 5 mm

CST results:
A. Polemi and S. Maci

Metasurfaces

- Surface-waves supporting metasurfaces:

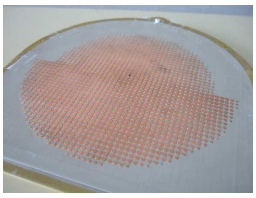

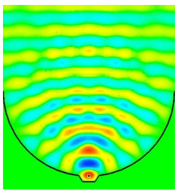

- Metasurface transmitarrays:

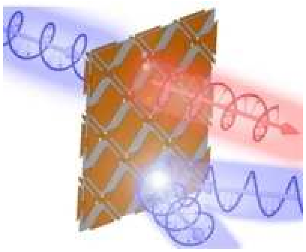

Picture: Anthony Grbic

Transparent and opaque metasurface boundary conditions

- Opaque (one-sided) surface impedance formulation:

$$\hat{n}\times\mathbf{E}^{+} = \hat{n}\times\left[\overline{\overline{Z}}_{surf}\cdot\left(\hat{n}\times\mathbf{H}^{+}\right)\right]$$

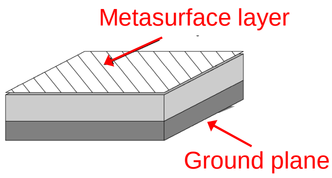

- Transparent (penetrable) surface impedance formulation:

$$\hat{n}\times\mathbf{E}_{av} = \hat{n}\times\left[\overline{\overline{Z}}_{surf}\cdot\left(\hat{n}\times\left(\mathbf{H}^{+}-\mathbf{H}^{-}\right)\right)\right]$$

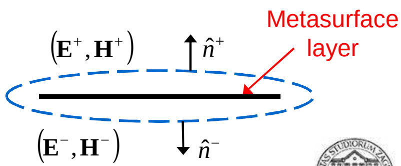

Analysis of metasurface structures
Surface impedance approach

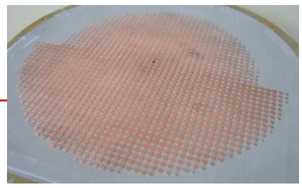

- Parameters of each patch are determined using a code for infinite periodic structure (or by measurements).
- We assume that each patch belong to infinite periodic array enviroment (local periodicity approach) which is reasonabe assumption if the changes of the neighboring patch dimensions are not too big.
- Admittance of metasurface structure is determined from reflection coefficient Γ (calculated or measured):

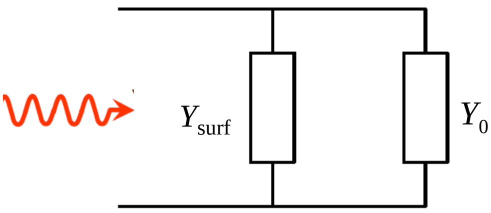

$$Y_{surf}^{TM} = Y_0^{TM}\frac{-2\Gamma^{TM}}{1+\Gamma^{TM}}$$

$$Y_{surf}^{TE} = Y_0^{TE}\frac{-2\Gamma^{TE}}{1+\Gamma^{TE}}$$

Surface impedance approach

- Shapes for which asymptotic formulas can be found in literature:

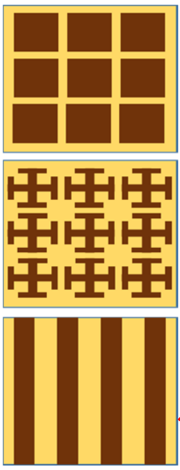

For plane wave propagating along the strips
$(k_z = k_0 \cos\theta)$:

$$Z^{TM}_{surf} = j\frac{k_0\eta_0}{2\pi} P \log\left(\csc\left(\frac{\pi W}{2P}\right)\right)\left(1+\frac{k_z^2}{k_{eff}^2}\right)$$

$$Y^{TE}_{surf} = j\frac{\pi\eta_0}{k_0(1+\varepsilon_r)} P \log\left(\csc\left(\frac{\pi W}{2P}\right)\right)\left(1+\frac{k_z^2}{k_{eff}^2}\right)$$

Surface impedance approach

- Comparison of different patch/line elements:

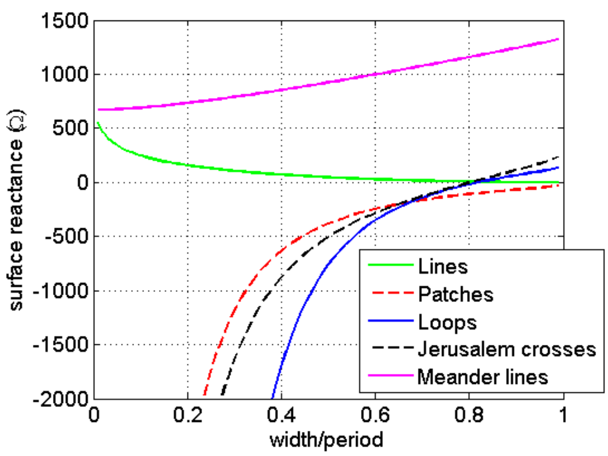

Metasurface transmitarrays
Application: Mantle cloak

Mantle cloak:

- The optimum value of metasurface reactance is obtained by performing a parametric sweep and calculating the minimum total scattered field:

$$Z_{surf} = -j \cdot 12.23\Omega$$

- The metasurface is realized using different types of periodic structures (patches, Jerusalem crosses).

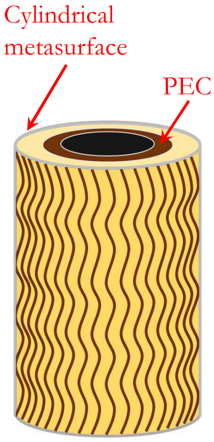

ρ_{PEC} = 10 mm
ρ_{meta} = 10.5 mm
ε_r = 20
f = 3 GHz

Metasurface transmitarrays
Application: Mantle cloak

- Mantle cloak:

$$Z_{surf} = -j \cdot 12.23\Omega$$

- Without cloak

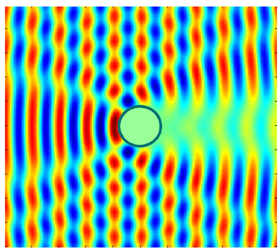

- With cloak

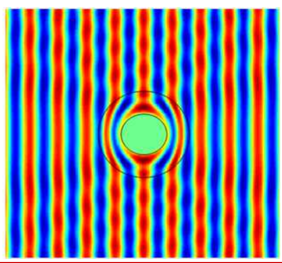

Metasurface transmitarrays
Application: Mantle cloak

- Mantle cloak:

$$Z_{surf} = -j \cdot 12.23\Omega$$

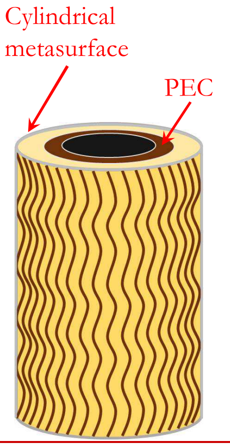

Reduction in scattered field
(total scattering width)

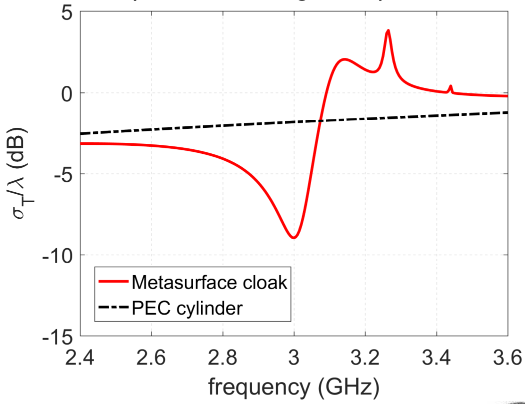

Results – mantle cloak

- Reduction in scattered field (total scattering width):

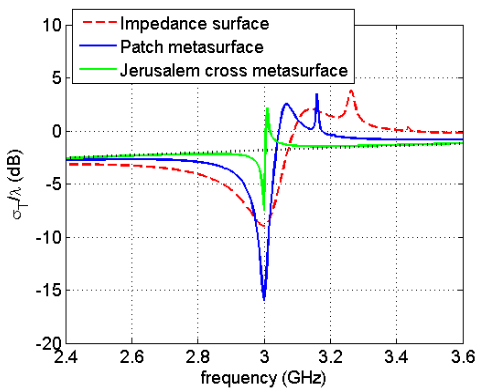

Two metasurface realizations:

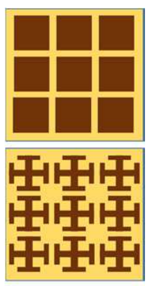

- Dimensions are optimized to obtain the minimum total scattering width.

Results – mantle cloak

- Dependancy of surface impedance on angular mode:

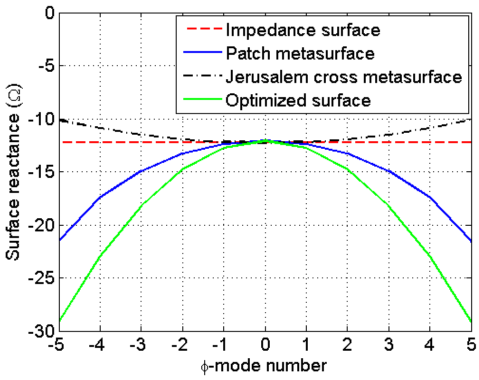

Two metasurface realizations:

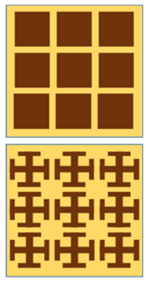

- Note: the impedance profile of the patch metasurface is rather close to the optimal case

Surface-waves supporting metasurfaces
Application: Luneburg lens antenna

- Luneburg lens based antenna:
  - the antenna should be designed in a way that it uses maximum lens area to achieve maximum radiating aperture:

Entire lens is excited by a small monopole with a backreflector

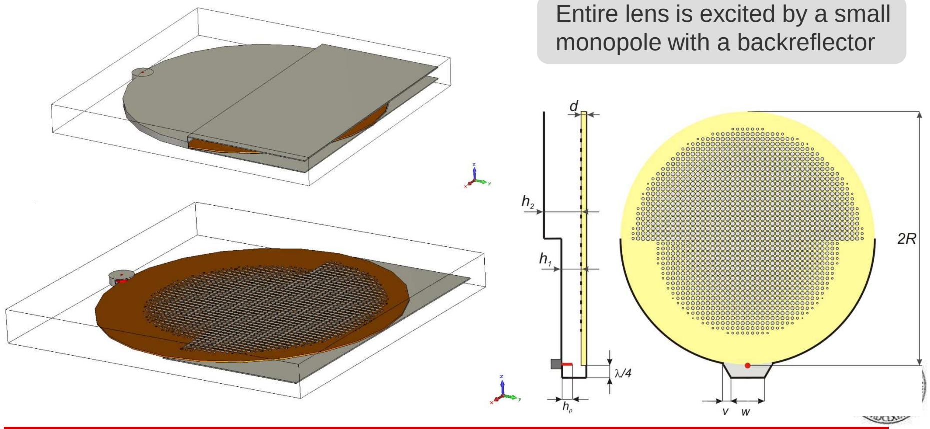

Surface-waves supporting metasurfaces
Application: Luneburg lens antenna

- Transverse resonance method:

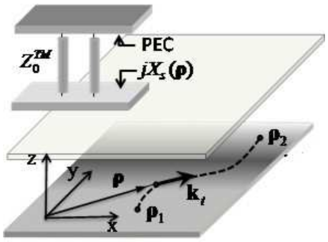

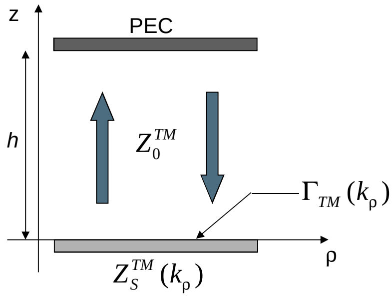

Dispersion relation: $Z_S^{TM}(k_\rho) = -jZ_0^{TM}\tan(k_z h)$

$$Z_S^{TM} = jX_S \qquad Z_0^{TM} = \eta_0 k_z / k_0 \qquad k_z = -j\alpha_z$$

$$\Rightarrow \quad X_S = \eta_0 \frac{\alpha_z}{k_0}\tanh(\alpha_z h) \qquad n_{eq} = \sqrt{1+\left(\frac{\alpha_z}{k_0}\right)^2}$$

Surface-waves supporting metasurfaces
Application: Luneburg lens antenna

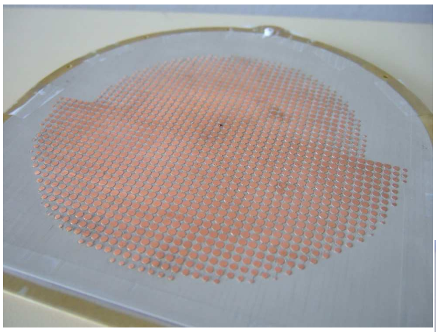

Prototype of the two step lens antenna:

Surface-waves supporting metasurfaces
Application: Luneburg lens antenna

Designed for
h_1 = 2.3 mm

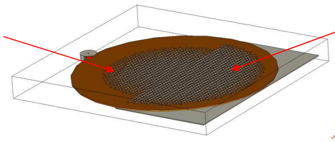

Designed for
h_2 = 5.75 mm

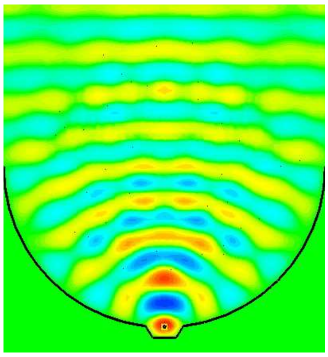

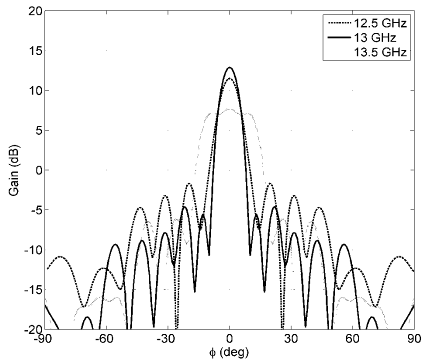

Outline

- Motivation
- Canonical surfaces, EBG surfaces, soft and hard surfaces
- Applications
- Modelling of EM surfaces
- **G1DMULT and G2DMULT algorithms**
- Story about cloaking

Calculation of Green's functions

Analytic methods:

- need less computer time
- if the topology of the problem is changed, the new Green's functions must be derived
- convenient for problems where the topology of the structure is fixed.

Numerical methods:

- more general
- need more computer time
- convenient for problems where the topology of the structure is changeable.

Algorithms for calculating Green's functions

G1DMULT algorithm:

- algorithm calculates Green's functions in spectral domain
- planar, circular-cylindrical and spherical structures
- multilayer structures

Recently, we have extended the G1DMULT algorithm to include calculation of Green's functions of structures containig metasurface layers.

Theoretical background

The G1DMULT algorithm is based on:

- Transformation of the 3D EM problem into the spectral-domain, and by this to transform the 3D problem into a spectrum of 1D problems.
- Implementation of the Love's equivalence theorem in order to analyze multilayer structures with arbitrary number of layers.

Structure of G1DMULT algorithm

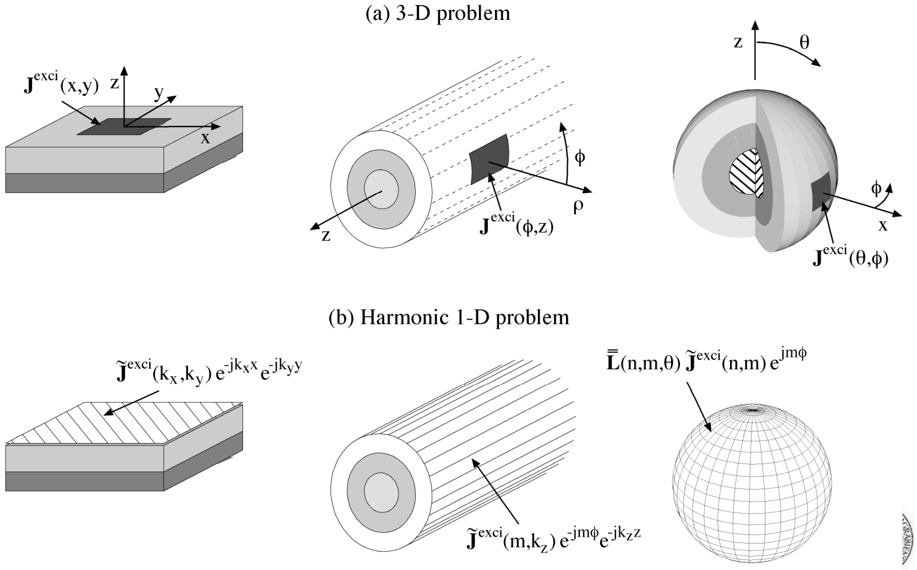

(c) Definition of material boundaries and regions

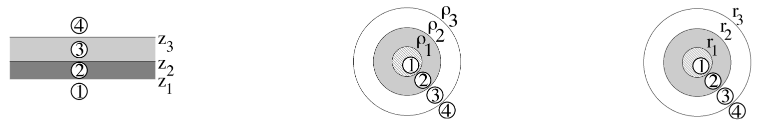

(d) Equivalent problem of region j

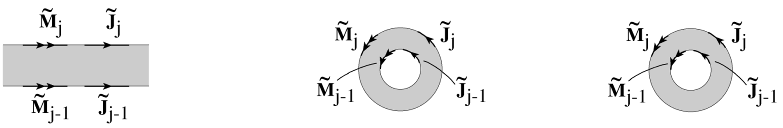

(e) Basic homogeneous harmonic 1-D field problem

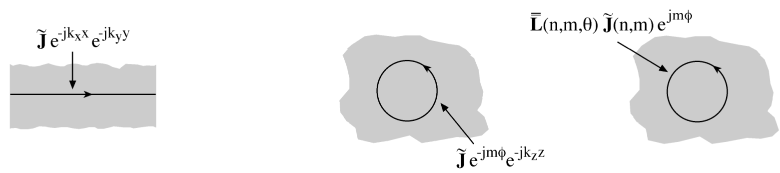

Structure of G1DMULT algorithm

- EM field inside each layer (e.g. electric field):

$$\tilde{\mathbf{E}}_j = \tilde{\bar{\bar{\mathbf{G}}}}^{homo}_{EJ}\tilde{\mathbf{J}}^{eq}_{j-1} + \tilde{\bar{\bar{\mathbf{G}}}}^{homo}_{EJ}\tilde{\mathbf{J}}^{eq}_{j} + \tilde{\bar{\bar{\mathbf{G}}}}^{homo}_{EM}\tilde{\mathbf{M}}^{eq}_{j-1} + \tilde{\bar{\bar{\mathbf{G}}}}^{homo}_{EM}\tilde{\mathbf{M}}^{eq}_{j}$$
$$+ \tilde{\bar{\bar{\mathbf{G}}}}^{homo}_{EJ}\tilde{\mathbf{J}}^{exci}_{j} + \tilde{\bar{\bar{\mathbf{G}}}}^{homo}_{EM}\tilde{\mathbf{M}}^{exci}_{j}$$

region boundary

- Boundary conditions for each boundary:

$$\tilde{E}_{x,j+1} - \tilde{E}_{x,j} = 0, \qquad \tilde{E}_{y,j+1} - \tilde{E}_{y,j} = 0,$$
$$\tilde{H}_{x,j+1} - \tilde{H}_{x,j} = 0, \qquad \tilde{H}_{y,j+1} - \tilde{H}_{y,j} = 0.$$

region

Structure of G1DMULT algorithm

- Matrix inside G1DMULT:

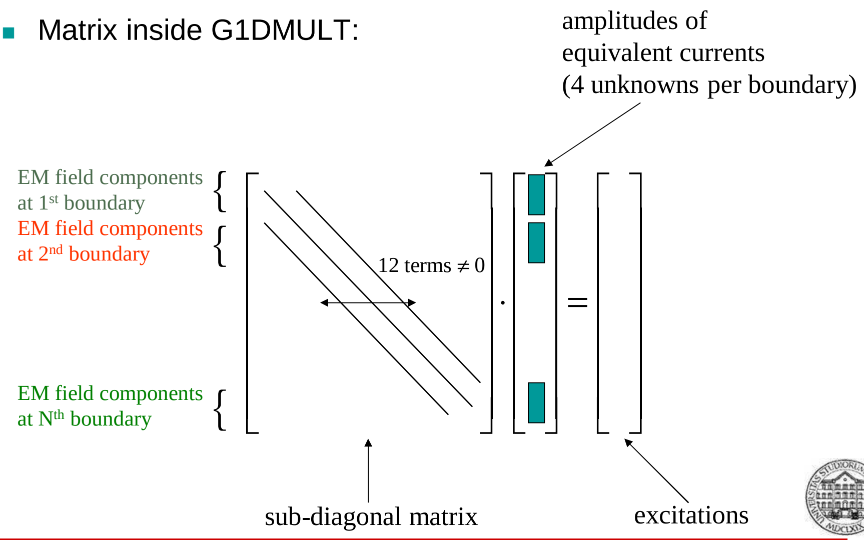

Transparent and opaque metasurface boundary conditions

- Opaque (one-sided) surface impedance formulation:

$$\hat{n}\times\mathbf{E}^+ = \hat{n}\times\left[\overline{\overline{Z}}_{surf}\cdot\left(\hat{n}\times\mathbf{H}^+\right)\right]$$

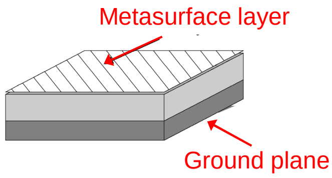

- Transparent (penetrable) surface impedance formulation:

$$\hat{n}\times\mathbf{E}_{av} = \hat{n}\times\left[\overline{\overline{Z}}_{surf}\cdot\left(\hat{n}\times\left(\mathbf{H}^+ - \mathbf{H}^-\right)\right)\right]$$

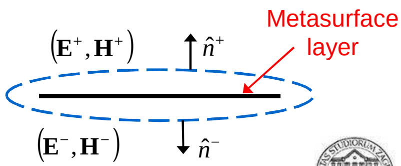

Implementation of opaque boundary conditions

- Opaque impedance boundary conditions:
  - Implementation of $\hat{n}\times\mathbf{E}^{+}=\hat{n}\times\left[\overline{\overline{Z}}_{surf}\cdot\left(\hat{n}\times\mathbf{H}^{+}\right)\right]$
  - The system of equations inside G1DMULT (for determining the equivalent currents at the layer boundaries) is reduced.

$$\boxed{\tilde{\mathbf{M}}^{eq}=-\hat{n}\times\left(\overline{\overline{Z}}_{surf}\cdot\tilde{\mathbf{J}}^{eq}\right)}$$

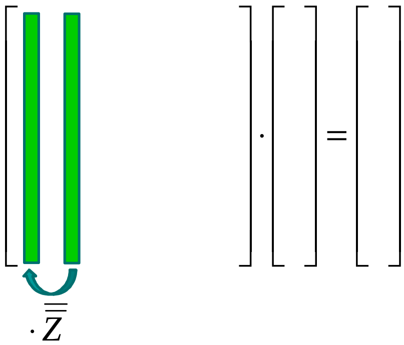

Implementation of transparent boundary conditions

- Model of a transparent (penetrable) metasurface layer suitable for implementation into the G1DMULT algorithm
  - Implementation of $\hat{n}\times\left(\mathbf{H}^{+}-\mathbf{H}^{-}\right)=\overline{\overline{Y}}_{surf}\cdot\mathbf{E}_{\tan}$

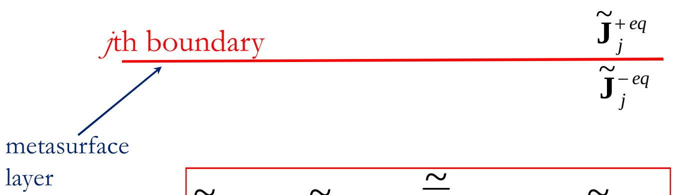

$$\boxed{\tilde{\mathbf{J}}_{j}^{-eq}=\tilde{\mathbf{J}}_{j}^{+eq}+\tilde{\overline{\overline{Y}}}_{surf}\cdot\left(\hat{n}\times\tilde{\mathbf{M}}_{j}^{eq}\right)}$$

Algorithms for calculating Green's functions

G2DMULT algorithm:

- Algorithm calculates Green's functions in spectral domain
- Multilayer structures
- Body-of-Revolution (BoR) structures
- Cylindrical structures with general cross-section

Recently, we have also extended the G2DMULT algorithm to include calculation of Green's functions of structures containig metasurface layers.

G2DMULT algorithm

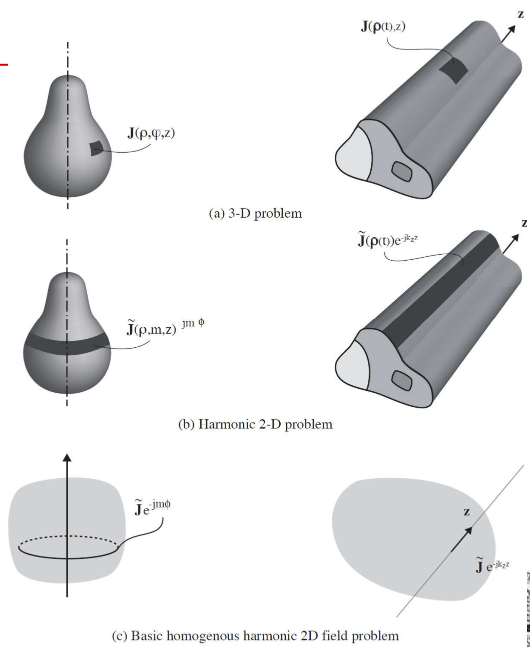

G2DMULT algorithm – Harmonic 2D problem

- The BoR surface is defined by its generating curve rotated about the BOR axis of symmetry

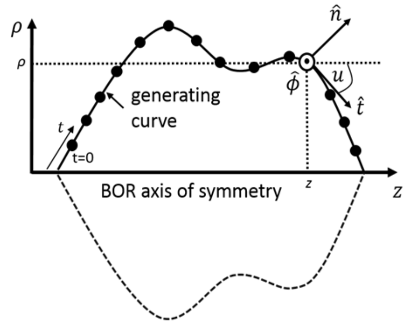

$$\hat{t} = \hat{\rho}\sin u + \hat{z}\cos u$$

$$\hat{n} = \hat{\phi}\times\hat{t} = \hat{\rho}\cos u - \hat{z}\sin u$$

G2DMULT algorithm – Harmonic 2D problem

- For each ϕ -harmonic we need to solve the MoM problem.
- Triangle (in *t*-direction) and pulse (in ϕ -direction) basis functions are used to apoproximate the surface currents:

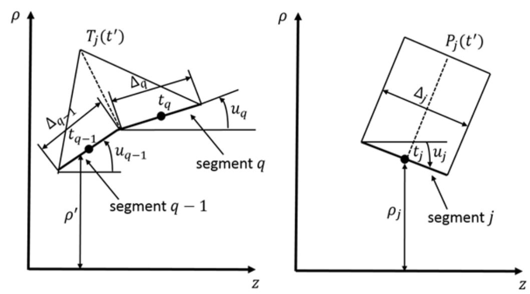

$$\mathbf{J}(\mathbf{r}') = \sum_{n=-\infty}^{\infty}\left\{\sum_{j=1}^{N_T}\alpha_{nj}^{T}\frac{T_j(t')}{\rho'}e^{jn\phi'}\hat{t}' + \sum_{j=1}^{N_P}\alpha_{nj}^{P}\frac{P_j(t')}{\rho_j}e^{jn\phi'}\hat{\phi}'\right\}$$

Flow chart of G1DMULT and G2DMULT algorithms

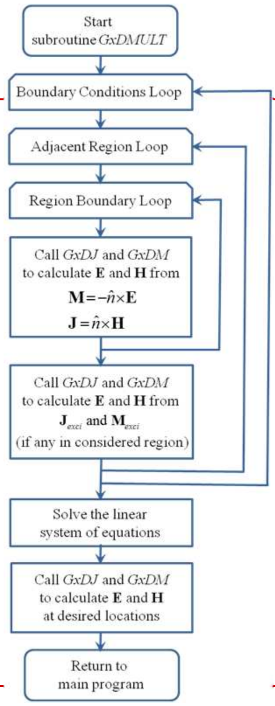

Outline

- Motivation
- Canonical surfaces, EBG surfaces, soft and hard surfaces
- Applications
- Modelling of EM surfaces
- G1DMULT and G2DMULT algorithms
- **Story about cloaking**

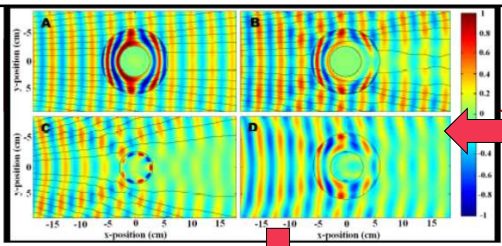

Schurig, Pendry at al 2006: Metamaterials graded index cloak

published in Sciencexpress. *Rated as the Fifth largest breakthrough in science in 2006.*

Appeared in media all over the world after this CNN report.

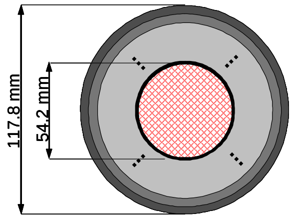

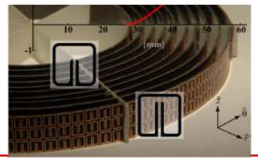

First experimental cloak realization

- Schurig, Pendry *at al.* (2006): Metamaterials graded index cloak :

Simplified cloak

Ideal case

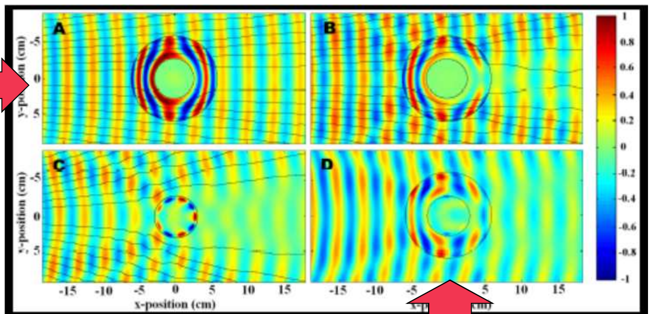

Measurements

- There was no measure how good the cloak is!

Question: how to characterize a cloak?

- **Scattering width σ_{2D}** – angular dependence of scattered field.
- **Total scattering width σ_T** (total SW) – ratio of the scattered power per unit length and the intensity of the incident Poynting vector.
- **Total SW reduction** – ratio of the total SW of the object we try to hide (PEC cylinder in our case) and the achieved total SW for the observed case with a cloak present.
  - Could also be considered as “invisibility gain”.

Natural way of designing devices

Concept development

↓

Device development

↓

Practical realization

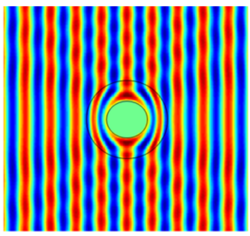

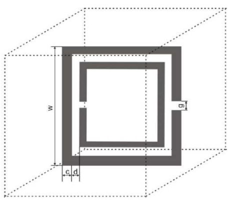

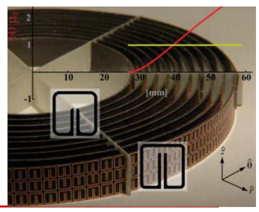

Natural way of designing devices

- Natural question that was posed with first cloak experiments:
  - What is the best possible cloak that can be realized using metamaterial approach?
- In order to give the answer to this question we have studied cylindrical cloaks realized from anisotropic homogeneous materials
  - Design of the cloaks always starts with the analysis of structures built from homogeneous material layers.
  - Practical realization is actually a metamaterial realization of an ideal structure made from homogeneous layers.
  - Therefore, the practical realizations have always worse properties comparing to ideal structure.

Ideal invisible cloak layout

- For the cloak design the used coordinate transformation compresses free space from the cylindrical region $0 < \rho < b$ into the annular region $a < \rho' < b$.

$$\rho' = a + \frac{b-a}{b}\rho, \qquad \phi' = \phi, \qquad z' = z$$

- This transformation leads to expressions for permittivity and permeability tensors (fully anisotropic structure):

$$\varepsilon_{\rho\rho} = \mu_{\rho\rho} = \frac{\rho - a}{\rho}$$

$$\varepsilon_{\phi\phi} = \mu_{\phi\phi} = \frac{\rho}{\rho - a}$$

$$\varepsilon_{zz} = \mu_{zz} = \left(\frac{b}{b-a}\right)^2 \frac{\rho - a}{\rho}$$

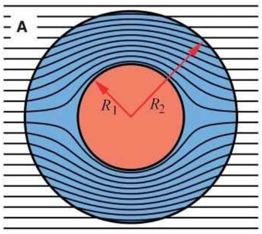

Reference: J. B. Pendry, D. Schurig, and D. R. Smith, Science, 2006.

TM_z cloak layout

- How to simplify the cloak design?
- For TM_z polarization and normal incidence the following products should not be modified:

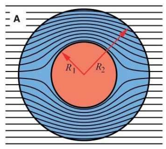

$$\varepsilon_{zz}\mu_{\rho\rho} = \left(\frac{b}{b-a}\right)^2 \left(\frac{\rho-a}{\rho}\right)^2 \qquad \varepsilon_{zz}\mu_{\phi\phi} = \left(\frac{b}{b-a}\right)^2$$

- In order to simplify metamaterial design, the following structure is proposed (with only $\mu_{\rho\rho}$ as a function of radius):

$$\varepsilon_{zz} = \left(\frac{b}{b-a}\right)^2 \qquad \mu_{\rho\rho} = \left(\frac{\rho-a}{\rho}\right)^2 \qquad \mu_{\phi\phi} = 1$$

- Note that such a design is suitable only for TM-polarization!

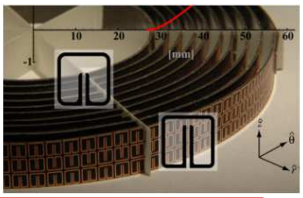

Reference: D. Schurig et al., Science, 2006.

Simplified invisible cloak layout

Ideal cloak	TM cloak	TE cloak
$\varepsilon_{\rho\rho} = \mu_{\rho\rho} = \frac{\rho-a}{\rho}$	$\mu_{\rho\rho} = \left(\frac{\rho-a}{\rho}\right)^2$	$\varepsilon_{\rho\rho} = \left(\frac{b}{b-a}\right)^2 \left(\frac{\rho-a}{\rho}\right)^2$
$\varepsilon_{\phi\phi} = \mu_{\phi\phi} = \frac{\rho}{\rho-a}$	$\mu_{\phi\phi} = 1$	$\varepsilon_{\phi\phi} = \left(\frac{b}{b-a}\right)^2$
$\varepsilon_{zz} = \mu_{zz} = \left(\frac{b}{b-a}\right)^2 \frac{\rho-a}{\rho}$	$\varepsilon_{\rho\rho} = \left(\frac{b}{b-a}\right)^2$	$\mu_{zz} = 1$

Drawbacks of simplified cloaks

Three large restrictions of the simplified cloaks:

- The modified condition for constitutive parameters:

$$\varepsilon_{zz}\mu_{\rho\rho} = \left(\frac{b}{b-a}\right)^2 \left(\frac{\rho-a}{\rho}\right)^2 \qquad \varepsilon_{zz}\mu_{\phi\phi} = \left(\frac{b}{b-a}\right)^2 \qquad (\text{TM}_z \text{ cloak})$$

$$\mu_{zz}\varepsilon_{\rho\rho} = \left(\frac{b}{b-a}\right)^2 \left(\frac{\rho-a}{\rho}\right)^2 \qquad \mu_{zz}\varepsilon_{\phi\phi} = \left(\frac{b}{b-a}\right)^2 \qquad (\text{TE}_z \text{ cloak})$$

  works only for
  - one polarization
  - normal incidence
- Reflections from the air-cloak boundary drastically reduce quality of the cloak.

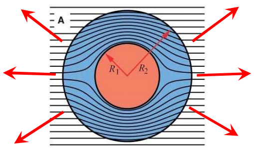

Invisible cloak layout

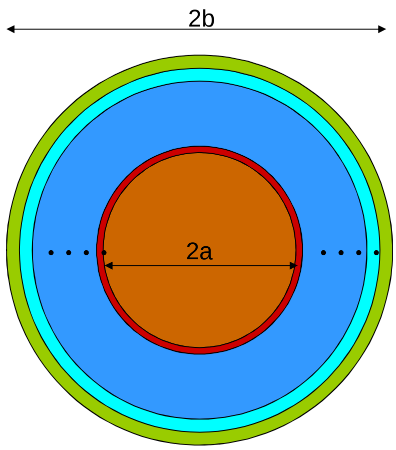

- The needed continuous radial variation of permeability and permittivity can be successfully approximated with *N* layers of constant permittivity.

a = 2.71 cm – cloak inner radius
b = 5.89 cm – cloak outer radius
f_0 = 8.5 GHz
(like in *Schurig et al's* cloak)

Schurig (TM_z) cloak – normal incidence

- PEC cylinder with a 10-layer realization of the Schurig cloak (f = 8.5 GHz, a = 2.71 cm, b = 5.89 cm):

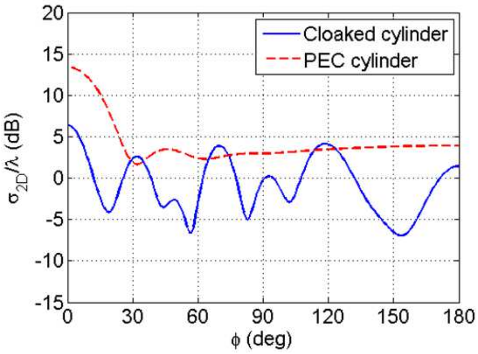

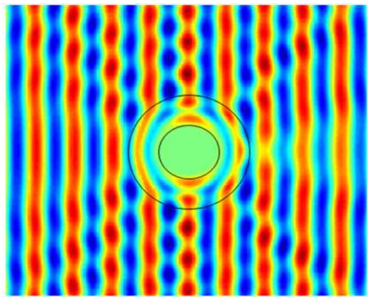

Schurig (TM_z) cloak - stepwise realization

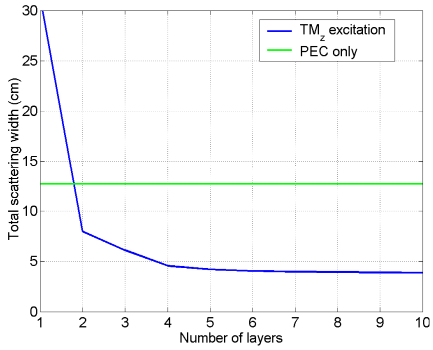

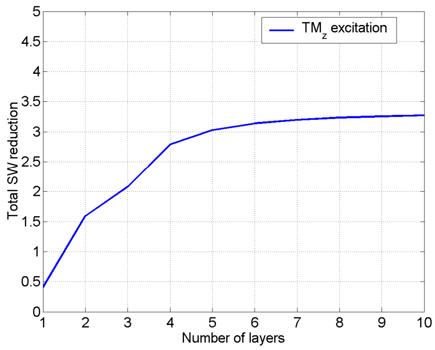

- Frequency: 8,5 GHz, inner radius: 2,71 cm, outer radius: 5,89 cm.
- The needed continuous radial variation of permeability can be successfully approximated with about 6 layers.
- For structures with more than 5 layers the “invisibility gain” is around 3.

Dispersion

- Extracted effective relative permeability (Hrabar et al., EuMC 2006)

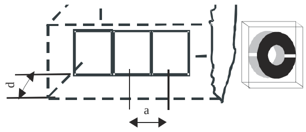

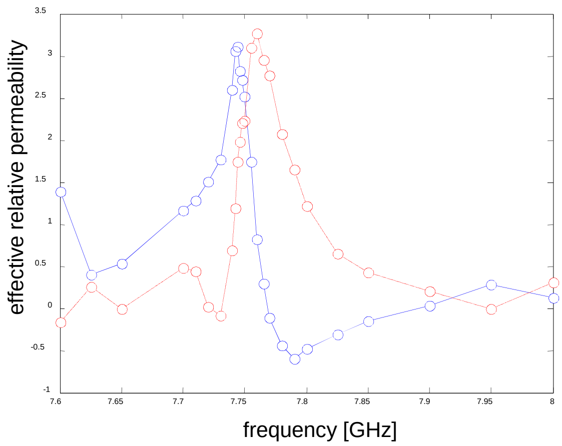

$$\mu_{eff} = 1 - \frac{f_{mp}^{\,2} - f_0^{\,2}}{f^2 - f_0^{\,2} - j\gamma f}.$$

From measurements:

$f_{mp} \approx 1.02\, f_0$

$\gamma \approx 0.012\, f_0$

Dispersion of the TM_z cloak

- Total SW versus frequency with dispersion included:

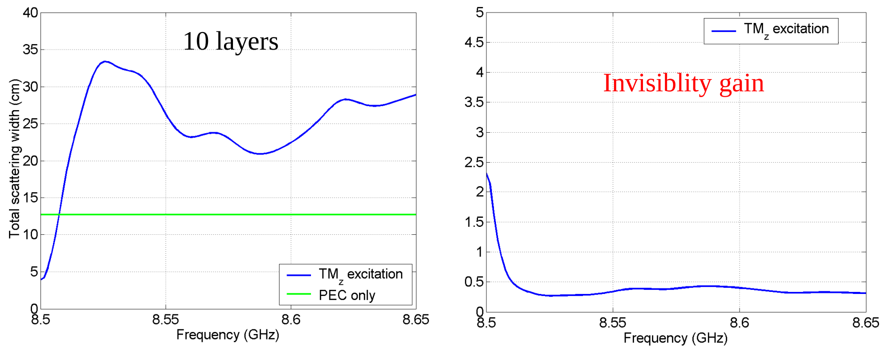

- The bandwidth of the TM_z cloak is approximately **0.24 %.**

Experimental verification of Schurig type of cloak

- Experiment at Duke University, Durham, USA
(N. Kundtz, D. Gaultney, D. R. Smith, New Journal of Physics, 2010).

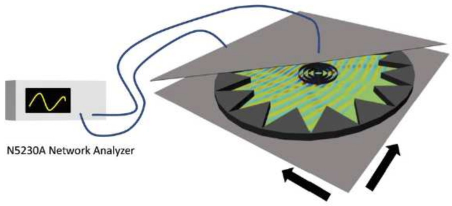

Figure 1. A 3D cutaway model of the waveguide apparatus with a cloak inside.

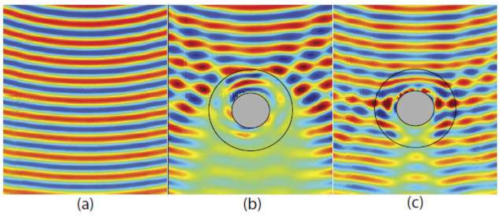

Experimental verification of Schurig type of cloak

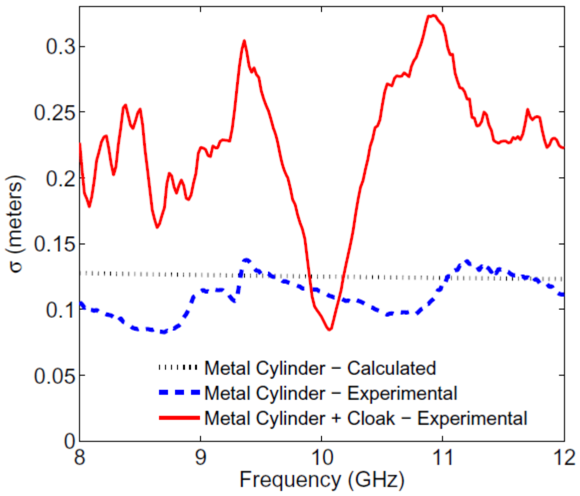

- **24% reduction in σ,**
- **Bandwidth of 230 MHz (2,3 %)**

N. Kundtz, D. Gaultney, D. R. Smith, New Journal of Physics, 2010.

Invisible cloak

- There was no measure how much is the cloak invisible!

Harry Potter wearing an invisibility cloak.

H. C. Andersen's fairy tale: The Emperor's new clothes were fake.

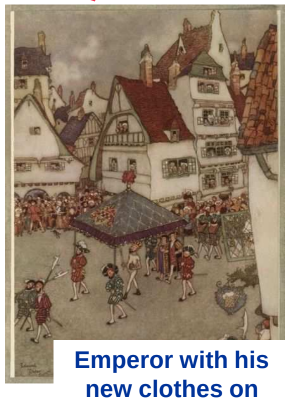

Emperor with his new clothes on

Reference: P.-S.Kildal, A. Kishk and Z. Sipus, IEEE AP Symposium 2007.

Improvement – mantle cloak

- Mantle cloak:

The optimum value of metasurface reactance is obtained by performing a parametric sweep and calculating the minimum total scattered field.

In this example:

$$Z_{surf} = -j\cdot 12.23\Omega$$

- Without cloak

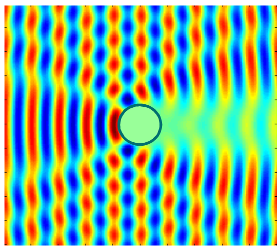

- With cloak

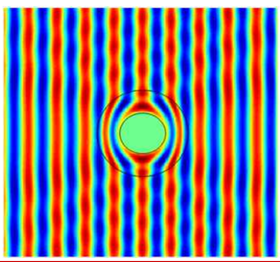

Improvement – mantle cloak

- Reduction in scattered field (total scattering width):

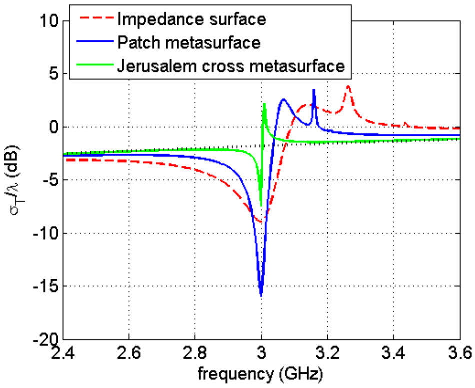

Two metasurface realizations:

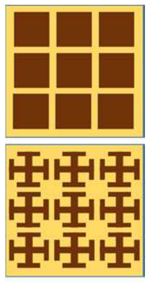

- Dimensions are optimized to obtain the minimum total scattering width.

Hard struts and mantle cloaks

Metamaterials Meeting Industrial Products: A Successful Example in Italy

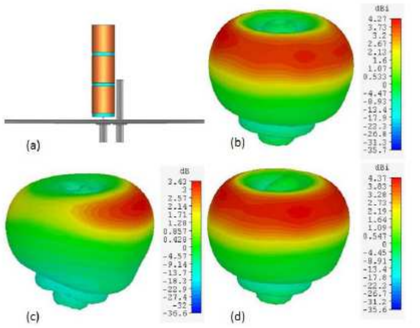

Fig. 3. (a) Schematic view of the designed antenna system consisting of two monopole radiators and a cloak surrounding the LTE monopole. (b) 3D realized gain pattern of the isolated UMTS antenna at f_{UMTS}. (c) 3D realized gain pattern of the UMTS antenna in the uncloaked scenario at f_{UMTS}. (d) 3D realized gain pattern of the UMTS antenna in the cloaked scenario at f_{UMTS}.

- IEEE Aps Symposium 2016 (G. Guarnieri et al.)
- The best invention award in Italy for 2015.

Hard struts and mantle cloaks

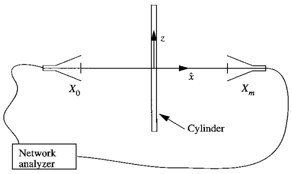

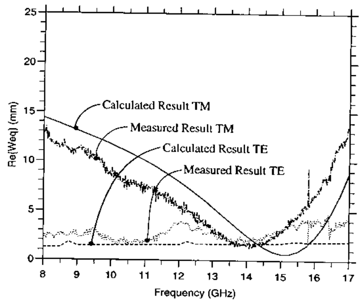

Picture: P.-S. Kildal

Summary

- Natural way of designing devices:

Concept development
↓
Device development
↓
Practical realization